Science Translational Medicine
AAAS

Supplementary Materials for

Reactivation of the tumor suppressor PTEN by mRNA nanoparticles enhances antitumor immunity in preclinical models

Yao-Xin Lin *et al*.

Corresponding author: Omid C Farokhzad, ofarokhzad@bwh.harvard.edu;
Lin Mei, meilin7@mail.sysu.edu.cn; Hao Wang, wanghao@nanoctr.cn;
Jinjun Shi, jshi@bwh.harvard.edu

Sci. Transl. Med. **13**, eaba9772 (2021)
DOI: 10.1126/scitranslmed.aba9772

The PDF file includes:

Other Supplementary Material for this manuscript includes the following:

1. Materials and Methods

Materials Bis(2-hydroxyethyl) disulfide (BHD), 3-Methyladenine (3-MA), Rapamycin and cationic generation 0 (G0) ethylenediamine core-poly(amidoamine) (PAMAM) were purchased from Sigma-Aldrich. PTEN mRNA (modified with 5-methylcytidine and pseudouridine), enhanced green fluorescent protein mRNA (EGFP mRNA; modified with 5-methylcytidine and pseudouridine) and Cyanine 5 fluorescent dye-labeled EGFP mRNA (Cy5-mRNA; modified with 5-methylcytidine and pseudouridine modification) were purchased from TriLink Biotechnologies. ViraPower Lentiviral packaging mix was purchased from Thermo Fisher Scientific. D-luciferin-K^+ salt bioluminescent substrate was obtained from Perkin Elmer. Primary antibodies used in this work included the following: anti-p62 (ab155686), anti-PTEN (ab31392), anti-Calreticulin (CRT, ab2907), Alexa Fluor 488-labled Calreticulin antibody (CRT, ab196158) and anti-hemagglutinin (HA) tag antibody (ab20084), which were purchased from Abcam; anti-PD-1 (BE0146) and anti-CD8α (BE0061) were purchased from Bio X Cell; pro-caspase-3 (2353), cleaved caspase-3 (9661), mixed lineage kinase domain-like (p-MLKL, 37333), LC3-II (2775) and β-actin (3700) were purchased from Cell Signaling Technology. Phospho-receptor interacting protein kinase 1 (p-RIPK1, PA5-104645) and receptor interacting protein kinase 3 (p-RIPK3, PA5-105700) were purchased from Thermo Fisher Scientific. Cytokines and chemokines including interleukin (IL)-1α/β, IL-6, IL-10, IL-12p70, tumor necrosis factor (TNF)-α and TNF-β, interferon (IFN)-γ enzyme-linked immunosorbent assay (ELISA) kits were purchased from BioLegend.

Synthesis of cationic lipid compound (G0-C14). The cationic lipid-like molecule (G0-C14) was synthesized as we previously reported. In brief, generation 0 dendrimer (G0) ethylenediamine core-poly(amidoamine) (PAMAM) was mixed with 1,2 epoxytetradecane at a molar ratio of 1:7, and then 1,2 epoxytetradecane were added to the above mixture. The mixture was vigorously stirred for 2 days and separated on silica with gradient elution buffer (CH_2Cl_2 to 75:22:3 CH_2Cl_2/MeOH/NH_4OH).

2% agarose measuring mRNA loading. To assess the mRNA complexation ability of G0-C14 and its stability in an organic solvent (dimethylformamide, DMF), naked EGFP-mRNA or EGFP-mRNA complexed with G0-C14 (in varying weight ratios from 1 to 20) were incubated with or without DMF for 30 minutes. For mRNA samples in DMF, electrophoresis was run without extracting mRNA from DMF into aqueous solution. The volumes of samples were then adjusted with loading dye (Invitrogen) and run into an E-Gel 2% agarose (Invitrogen) gel for 30 minutes at 50 V. The ambion millennium markers-formamide (Thermo Fisher Scientific) was used as a ladder. Finally, the gel was imaged under ultraviolet light and the bands were analyzed.

Tumor cell culture. Mouse cancer cells (B10F10 and PTEN-Cap8) were purchased from American Type Culture Collection (ATCC). *Pten*-null mouse prostate cancer cell line (BMPC) was gift from Dr. Charles J. Bieberich. All cells were Dulbecco's Modified Eagle Medium (DMEM; ATCC), 10% fetal bovine serum (FBS; Gibco) and 1% penicillin/streptomycin antibiotic (Thermo Fisher Scientific). For PTEN-Cap8, the full medium included 25 μg/mL bovine pituitary extract (BPE), 5 μg/mL human recombinant insulin, and 6 ng/mL human recombinant epidermal growth factor (EGF). All cells were maintained in a cell-culture incubator with 5% CO_2 at 37 °C.

Cell transfection activity of mRNA-encapsulated NPs. To assess the cell transfection of NPs, EGFP mRNA-encapsulated NPs (EGFP mRNA@NPs) were prepared and PTEN-Cap8 cancer cells were seeded in confocal wells (Costar) at a density of 3×10^5 cells per well. When the cells attached to about 80% of the well, naked EGFP mRNA and EGFP mRNA@NPs were added at 0.5 μg/mL of EGFP mRNA. After incubation for 48 hours, the cells were washed with PBS, and EGFP expression was imaged using an Olympus microscope.

Real-time PCR. The RNA of mPTEN@NPs-treated tumor cells was extracted with the use of TRIZOL reagents per manufacturer's instructions, and then reverse-transcribed into cDNA using a QuantiTect Reverse Transcription Kit per manufacturer's instructions. RT-PCR was conducted to measure mRNA using the Rotor-Gene SYBR Green PCR Kit. The mRNA increase was normalized to GAPDH. All experiments were performed in triplicate. The fold-change in mRNA expression is shown relative to the group without treatment served as 0. Primers for *PTEN*: 5′-TTTGAGAGTTGAGCCGCTGT-3′ and 5′-ATGCTTTGAATCCAAAAACCTTACT-3′

Phospho-array analysis. A phospho-specific protein microarray (Full Moon Microsystems) was used to measure the extent of protein phosphorylation. The array experiment was performed by Wayen Biotechnology. The phosphorylation was calculated by phosphorylation ratio = phosphorylated value/unphosphorylated value.

Development of GFP-LC3 or luciferase transferred PTEN-Cap8 cells. 293T cells were first transfected with lentiviral vector plasmids of Lenti cytomegalovirus (CMV) Puro LUC encoding Luciferase using lipofectamine 2000 and then incubated for 48 hours. Next, supernatant with Luciferase lentivirus was harvested and added into PTEN-Cap8 cells. 8 μg/mL of Polybrene (Sigma-Aldrich) was added into the above cell culture medium. After transfection for 48 hours, 2 μg/mL of puromycin (Sigma-Aldrich) was used to select the Luciferase lentivirus-infected PTEN-Cap8 cells. For development of GFP-LC3 transferred PTEN-Cap8 cells, PTEN-Cap8 cells were directly transfected with plasmids encoding GFP-LC3 protein using lipofectamine 2000 and then incubated for 24 hours.

Biodistribution of mRNA NP in a tumor-bearing mouse model. For the biodistribution study, B16F10-bearing C57BL/6 female mice were used. In brief, 4×10^5 B16F10 cells were implanted subcutaneously on the right flank of mice to establish subcutaneous tumors. When the average tumor size had increased to ~200 mm^3, tumor-bearing mice were then received 200 μL of saline and Cy5-mRNA@NPs via tail vein injection at an mRNA dose of 15 μg per animal. 24 hours later, organs (heart, liver, spleen, lung, and kidney) and tumors were isolated and imaged with the Syngene PXi Imaging System.

In vivo toxicity. To evaluate the in vivo toxicity of PTEN mRNA NPs, C57BL/6 male mice (6 weeks old) were randomly divided into 3 groups (n = 3 per group) and intravenously injected with PBS, control NPs, or mPTEN@NPs at an mRNA dose of 700 μg/kg of mouse body weight. Blood was collected from the retroorbital vein 24 hours after the final injection. Aspartate aminotransferase (AST, Sigma-Aldrich), alanine aminotransferase (ALT, Sigma-Aldrich), and blood urea nitrogen (BUN, Arbor) were measured using assay kits according to the manufacturers' protocols. For histological examination, tumors and various organs (lung, heart,

liver, kidney, and spleen) were harvested 2 days after the final mPTEN@NPs injection (day 15) and fixed with 4% paraformaldehyde. The organs were then embedded in paraffin, sectioned into thin slices (~5 μm thick) and prepared and stained with H&E using assay kit (Vector Laboratories) according to the manufacturer's protocols.

2. Supplementary Figures and Captions

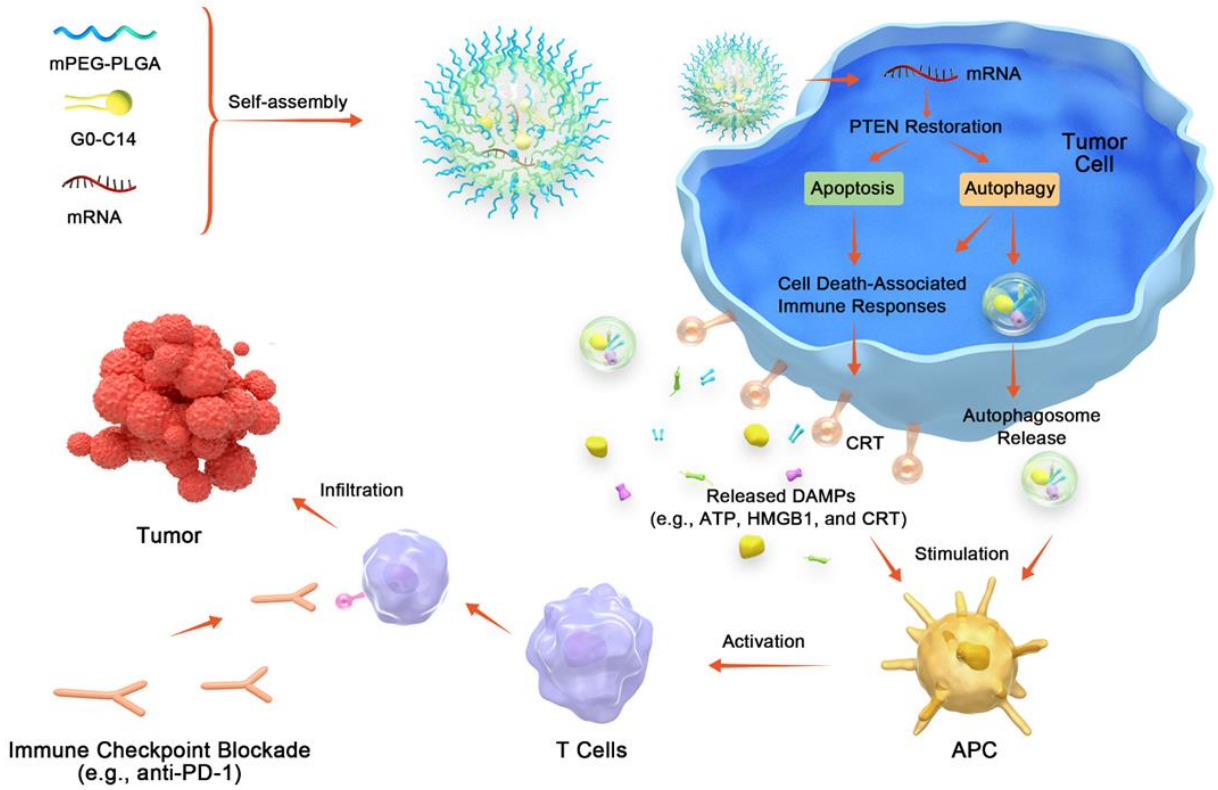

Fig. S1. Schematic of PTEN mRNA nanoparticles (NPs)-mediated cancer immunotherapy. The schematic illustrates PTEN restoration for inducing anti-tumor immune responses and sensitizing *PTEN*-null or mutated tumors to immune checkpoint blockade (ICB) therapy. mPTEN@NPs restored tumor cells' susceptibility to apoptosis and triggered cell death-associated immune activation *via* the release of damage-associated molecular patterns (DAMPs), such as calreticulin (CRT), ATP, and high mobility group box 1 (HMGB1), and *via* the induction of autophagy. Autophagy further promoted the release of DAMPs and autophagosomes, all of which would activate antigen presentation cells (APCs) and induce anti-tumor immunity.

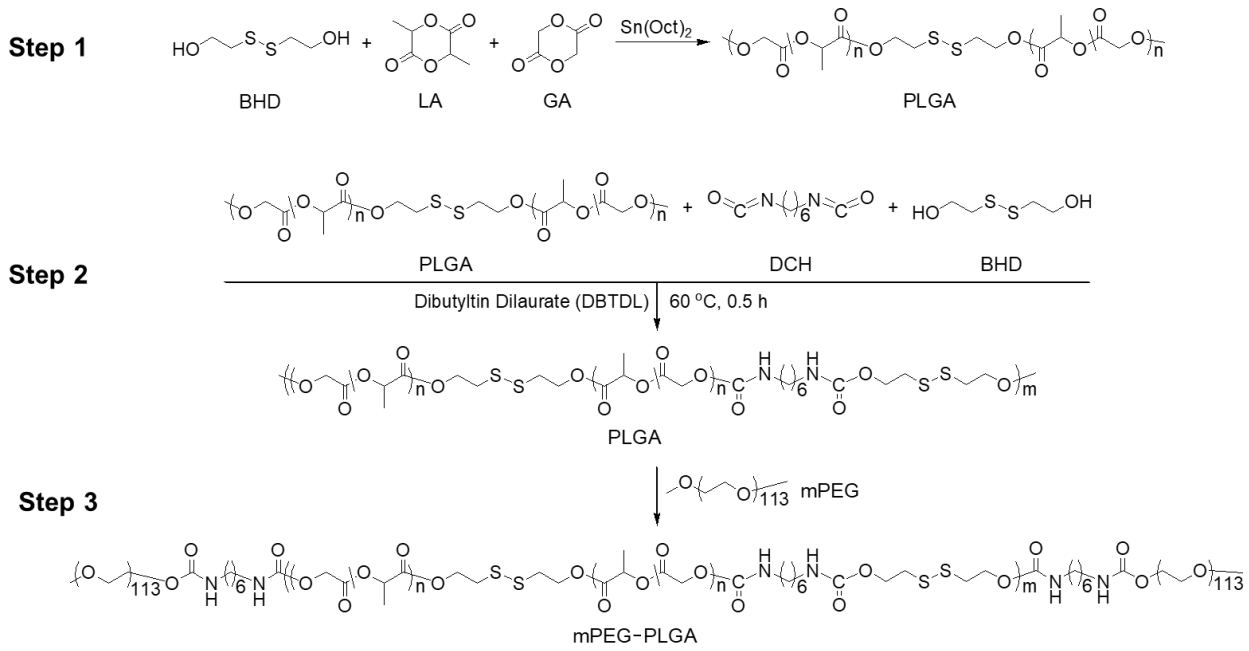

Fig. S2. Synthesis pathway for mPEG-PLGA.

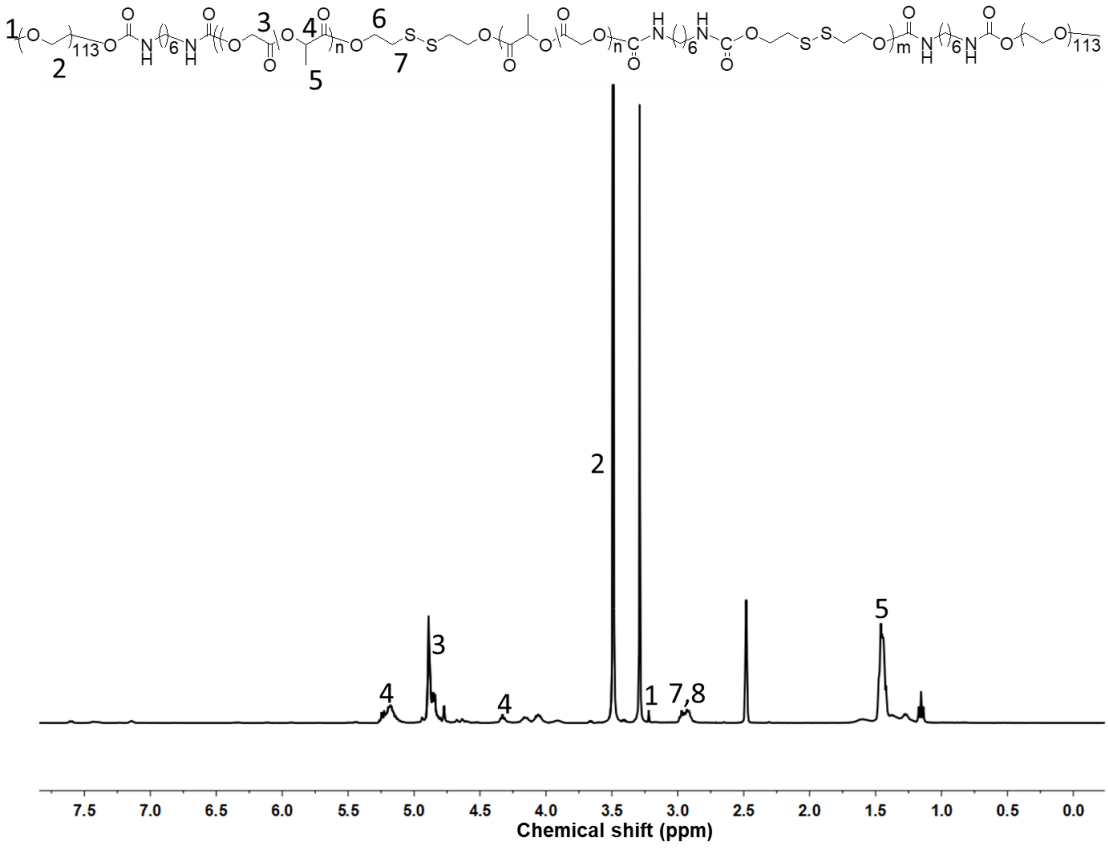

Fig. S3. ^{1}H NMR spectra of mPEG-PLGA in d_6-DMSO. The concentration of mPEG-PLGA in d_6-DMSO was 10 mg/mL. ppm stands for parts per million.

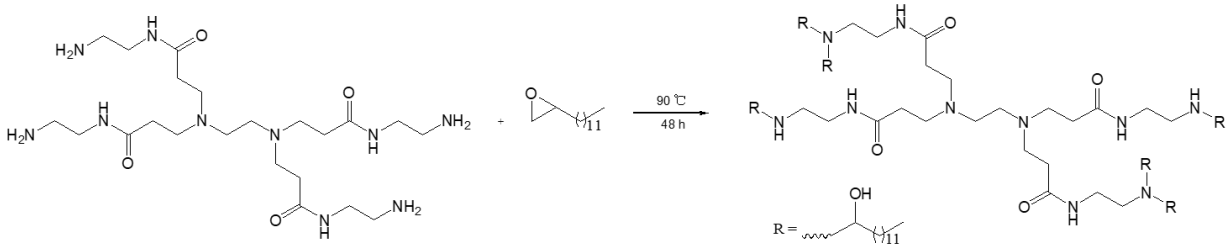

Fig. S4. Synthesis pathway for G0-C14.

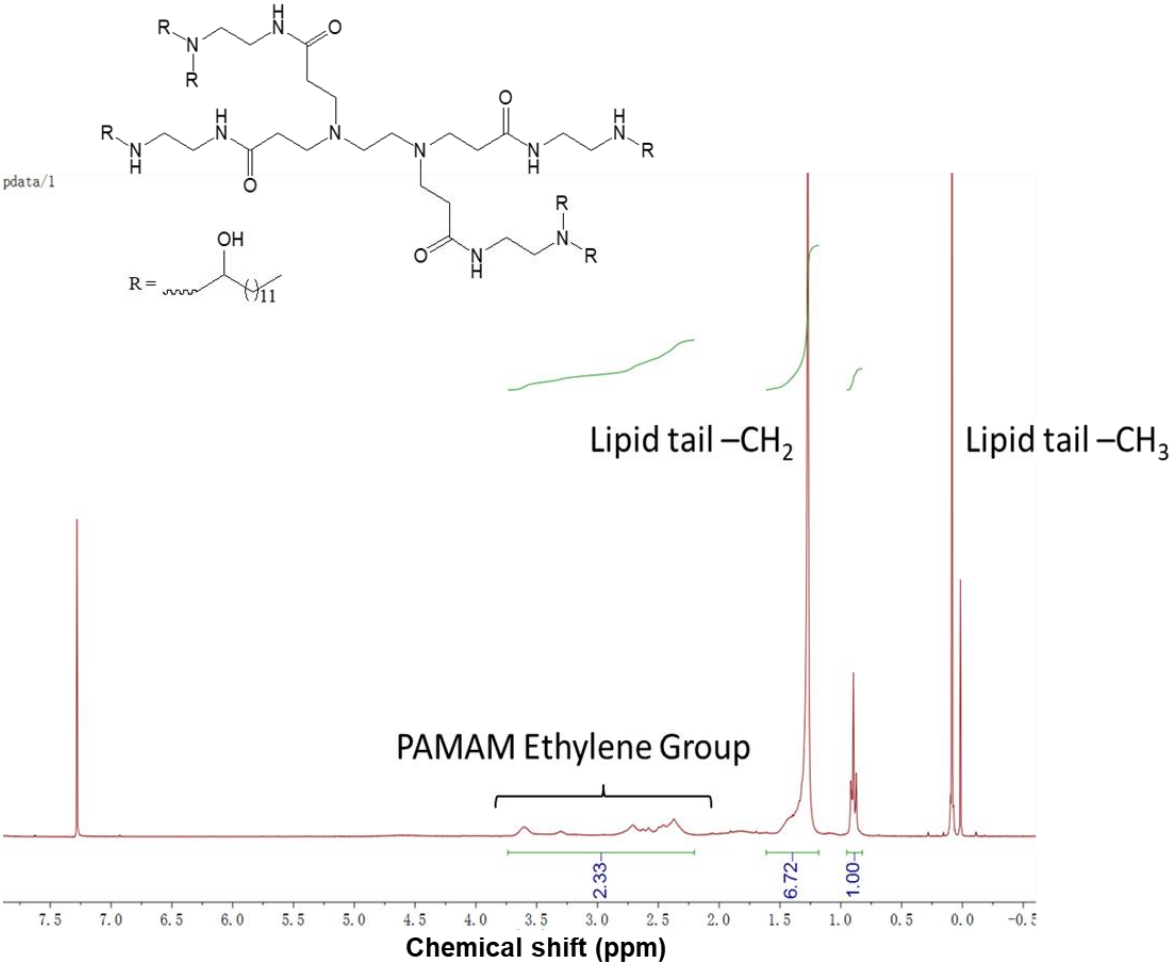

Fig. S5. ^{1}H NMR spectra of G0-C14 in chloroform. The concentration of G0-C14 in chloroform was 10 mg/mL.

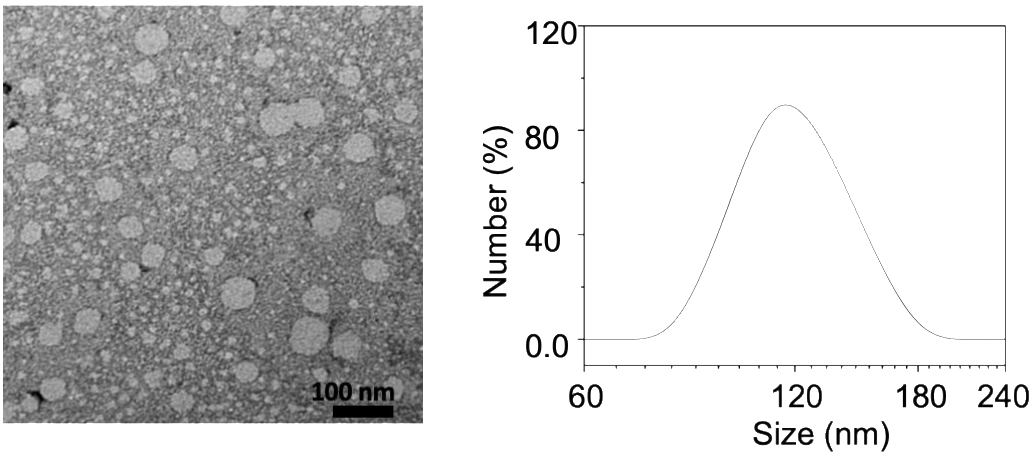

Fig. S6. TEM image of control NPs and the size distribution of NPs detected by DLS. The scale bar is 100 nm.

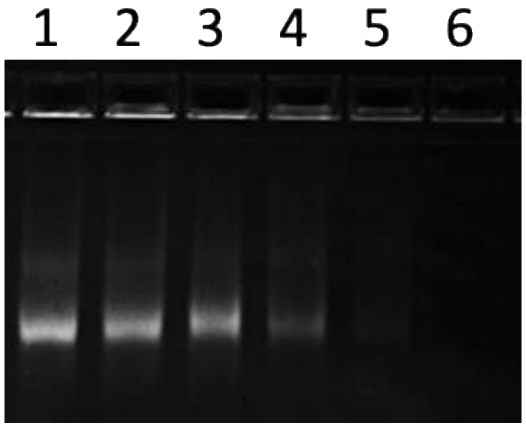

Fig. S7. RNA gel imaging for RNA loading detection. 1, naked mRNA (5 μg); 2, G0-C14/mRNA complexes with mass ratio of 3.2; 3, G0-C14/mRNA complexes with mass ratio of 6.25; 4, G0-C14/mRNA complexes with mass ratio of 12.5; 5, G0-C14/mRNA complexes with mass ratio of 25; 6, mPTEN@NPs with G0-C14/mRNA mass ratio of 25.

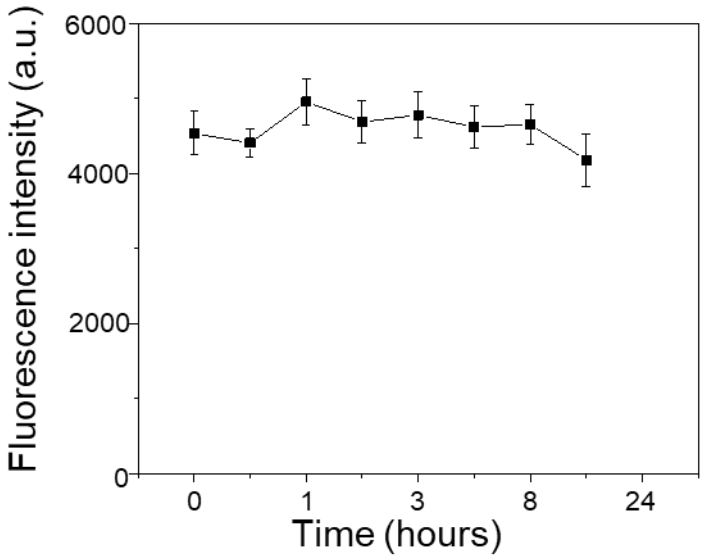

Fig. S8. Evaluation of the ability of the NPs to protect mRNA from RNase degradation. a.u.: arbitrary unit.

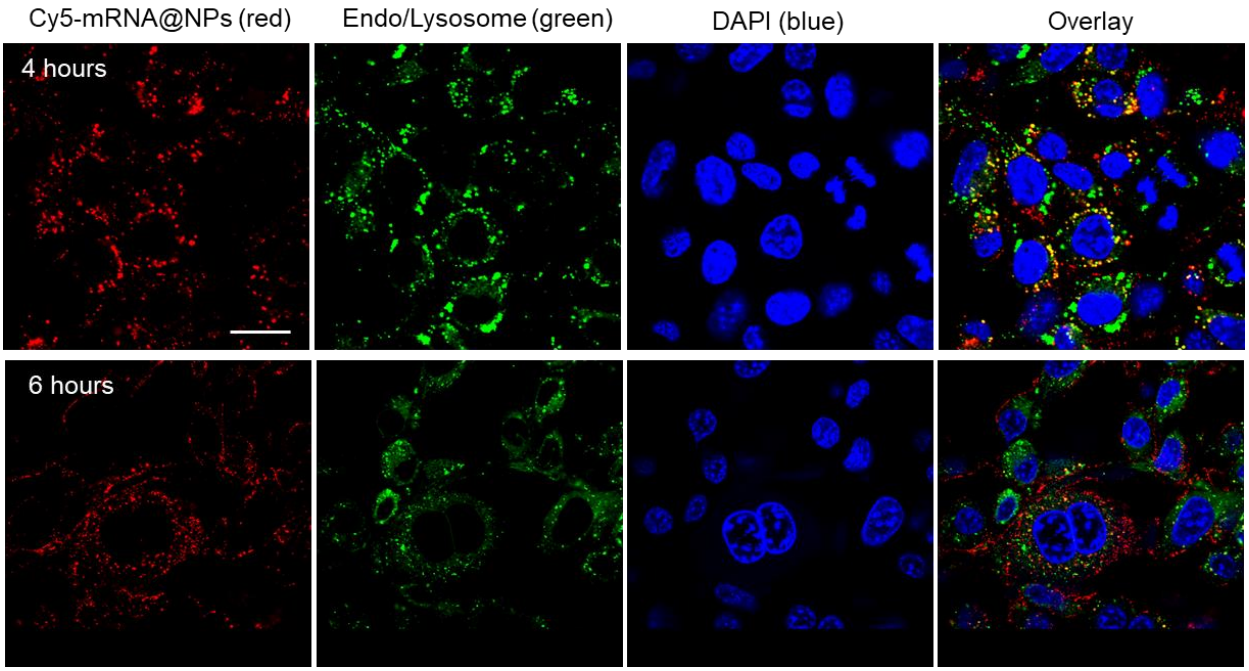

Fig. S9. The uptake and endo/lysosomal escape of Cy5-mRNA@NPs after 4 and 6 hours treatment. Cy5-mRNA@NPs (red), Endo/Lysosome (green), DAPI (blue). Scale bar, 20 μm.

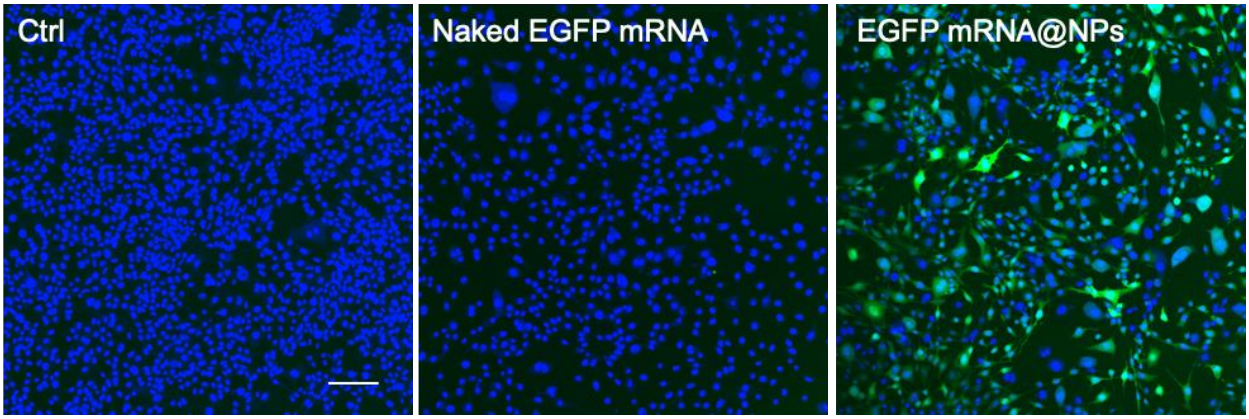

Fig. S10. Confocal laser scanning microscopy (CLSM) images of PTEN-Cap8 cells transfected with PBS (Ctrl), naked EGFP mRNA, and EGFP mRNA@NPs for 48 hours. EGFP (green), DAPI (blue). Scale bar, 100 μm.

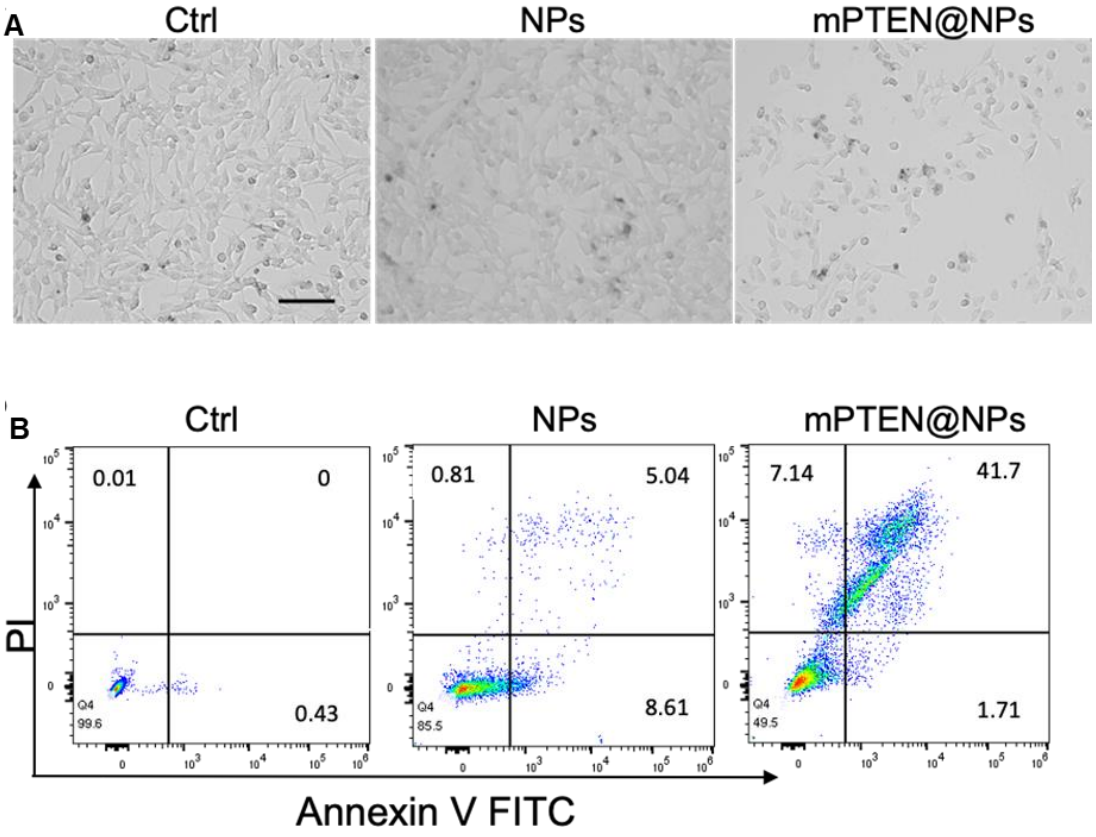

Fig. S11. Optical microscopy imaging and flow cytometry analysis on PTEN-Cap8 cells after treatment with PBS (Ctrl), control NPs, and mPTEN@NPs for 48 hours. (**A**) Optical microscopy imaging and (**B**) Apoptosis was measured by flow cytometry. FITC: Fluorescein isothiocyanate; PI: propidium iodide. Scale bar, 50 μm.

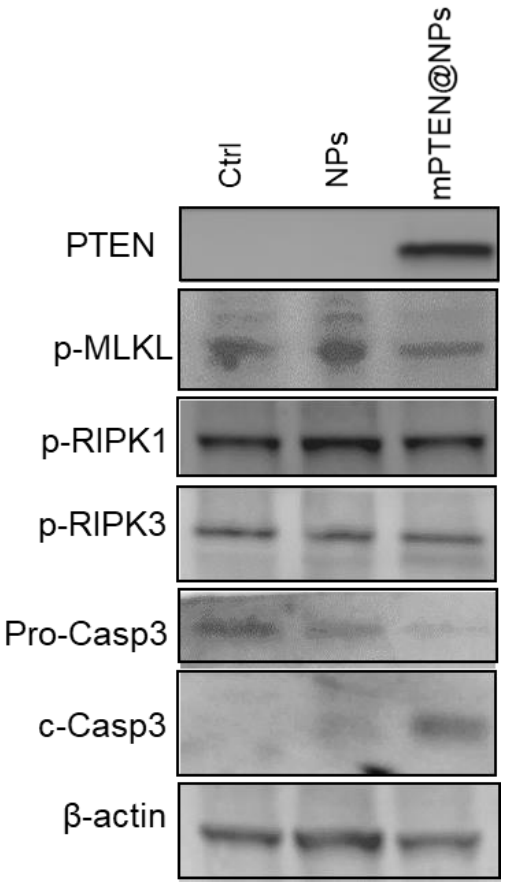

Fig. S12. Western blot analysis for cell death signaling. PTEN-Cap8 cells were treated with PBS (Ctrl), NPs, and mPTEN@NPs for 48 hours. PTEN, phosphatase and tensin homolog deleted on chromosome ten; Pro-Casp3, pro-caspase-3; c-Casp3, cleaved caspase-3; MLKL, mixed lineage kinase domain-like, RIPK1, receptor interacting protein kinase 1; RIPK3, receptor interacting protein kinase 3.

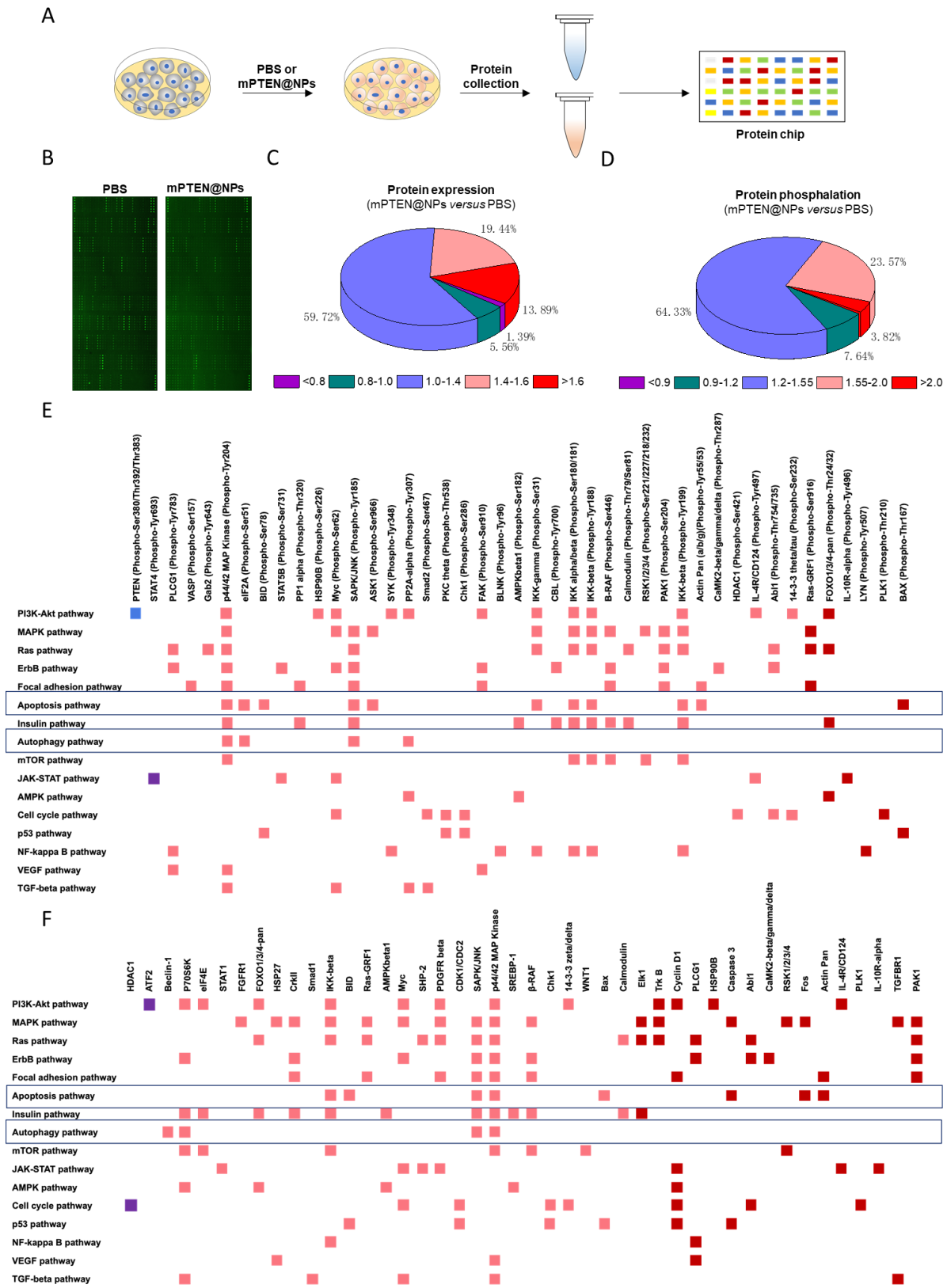

Fig. S13. Phospho-array analysis of protein phosphorylation in PTEN-Cap8 cells treated with PBS (Ctrl) or mPTEN@NPs. (**A**) Experimental design to detect the phosphorylated proteins in PTEN-Cap8 cells treated

with PBS and mPTEN@NPs for 48 hours. (**B**) Phospho-array for proteins. (**C and D**) Summary analysis of change of protein expression and phosphorylated proteins. The phosphorylation ratio = phosphorylated value/non-phosphorylated value. (**E and F**) Enrichment analysis of altered sites in 16 pathway signals.

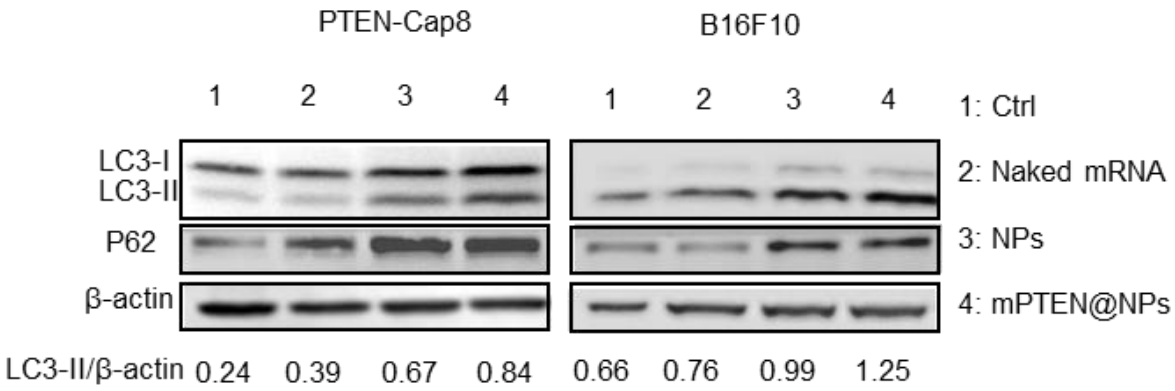

Fig. S14. Western blot analysis for autophagy signaling after mPTEN@NPs treatment. Cells were treated with naked mRNA, NPs, and mPTEN@NPs for 48 hours, and the cells without any treatment served as control (Ctrl). The bottom showed the quantitative analysis results for microtubule-associated protein 1-light chain 3-II (LC3-II) expression that were calculated by normalizing LC3-II protein band intensity at each condition to that of β-actin using ImageJ software.

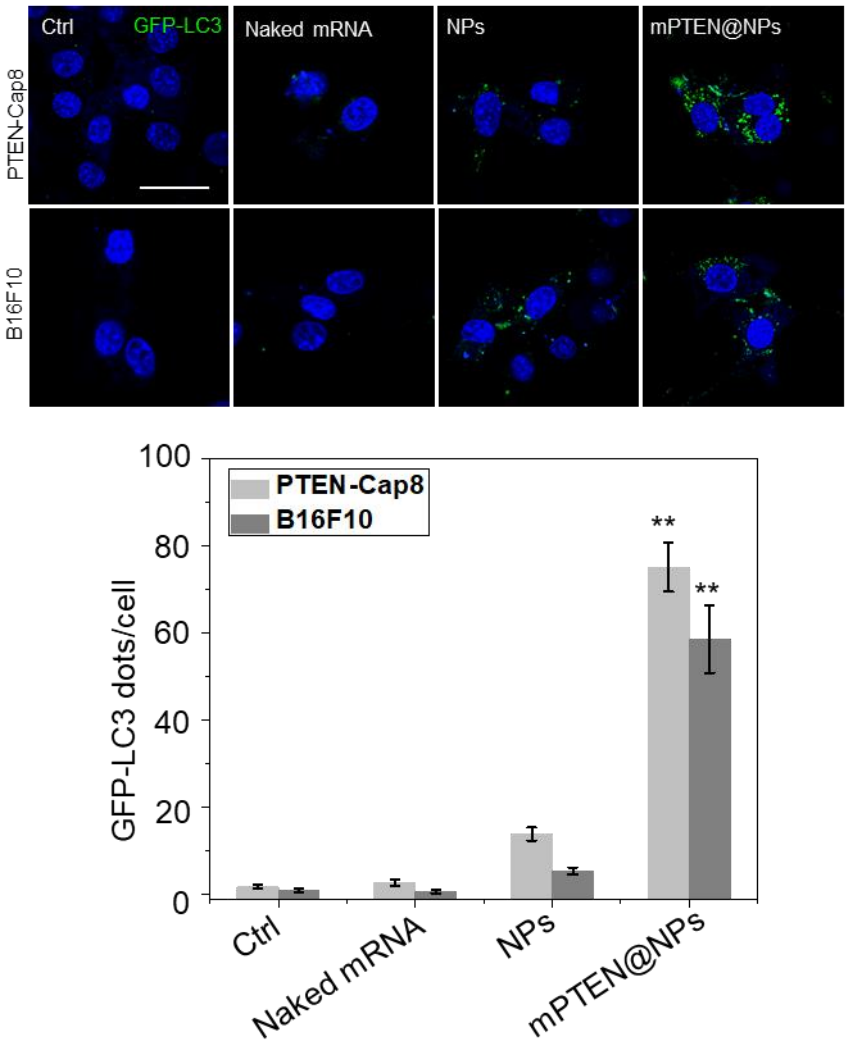

Fig. S15. CLSM imaging for cells transfected with GFP-LC3 and quantitative analysis of GFP-LC3 dots. Cells were transfected with GFP-LC3 plasmids and incubated for 24 hours, followed by treatment with PBS (Ctrl), naked mRNA, NPs, and mPTEN@NPs for 48 hours. Significance was calculated using a one-way ANOVA with a Tukey post-hoc test. **P < 0.01 versus Ctrl. Scale bar, 20 μm.

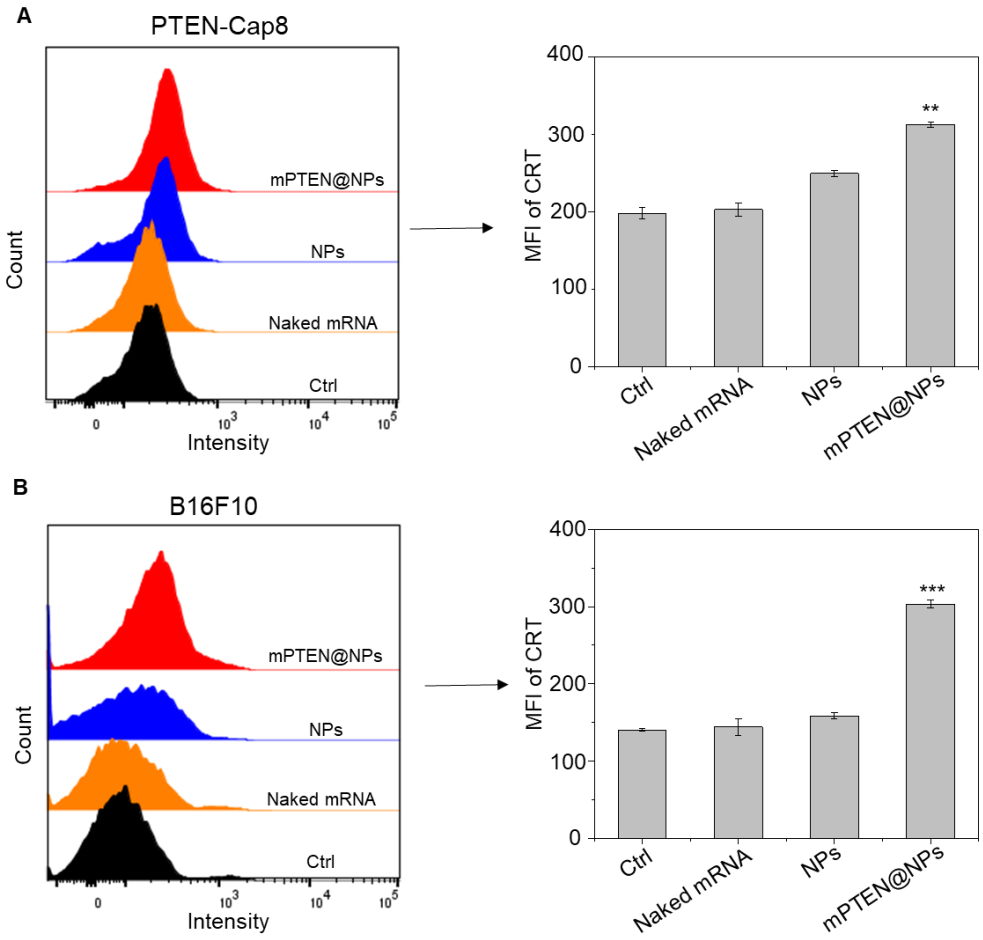

Fig. S16. mPTEN@NPs treatment increases calreticulin (CRT) abundance on the surface of tumor cells. (**A**) PTEN-Cap8 and (**B**) B16F10 cells were collected and stained with Alexa Fluor 488-labled CRT antibody after treatment with PBS (Ctrl), naked mRNA, NPs, and mPTEN@NPs for 48 hours. Data are presented as mean ± SD (n = 3 replicates per group), and analyzed by a one-way ANOVA with a Tukey post-hoc test. Statistical significance: **P < 0.01, ***P < 0.001 versus Ctrl. MFI: mean fluorescent intensity.

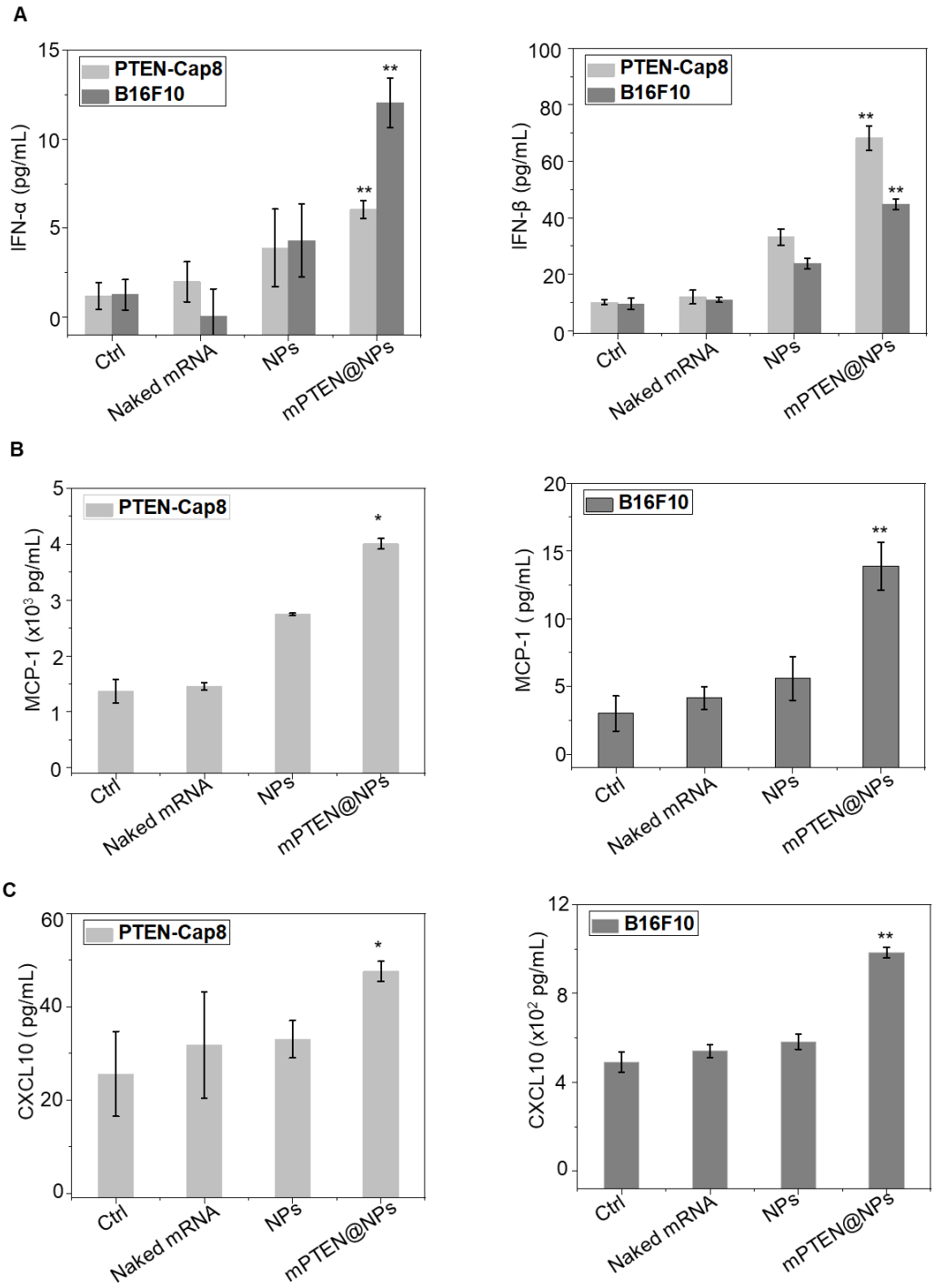

Fig. S17. Analysis of immunogenic cell death (ICD) markers in vitro. PTEN-Cap8 and B16F10 cells were treated with PBS (Ctrl), NPs, mPTEN@NPs and Cisplatin (100 μg/mL) for 48 hours. The cell culture medium was collected and measured with ELISA kits according to the manufacturer's instructions. (**A**) type I IFNs (IFN-α and IFN-β), (**B**) monocyte chemoattractant protein-1 (MCP-1), and (**C**) interferon γ-induced protein-10 (IP-10, also known as CXCL10). Data are presented as mean ± SD (n = 3 replicates per group), and analyzed by a one-way ANOVA with a Tukey post-hoc test. Statistical significance: *P < 0.05, **P < 0.01 versus Ctrl.

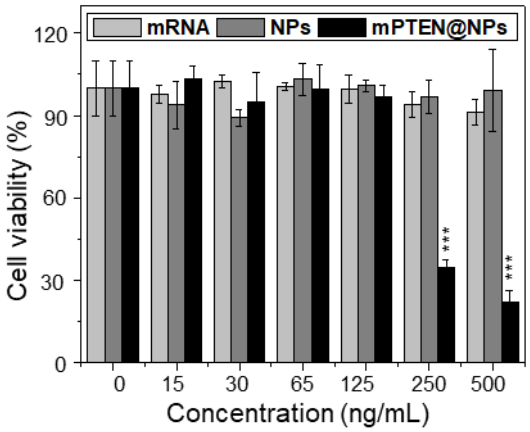

Fig. S18. **The effect of mPTEN@NPs on cell viability of *Pten*-null prostate (BMPC) tumor cells.** BMPC tumor cells were treated with naked mRNA, NPs and mPTEN@NPs for 48 hours. Data are presented as mean ± SD (n = 3 replicates per group), and analyzed by a one-way ANOVA with a Tukey post-hoc test. Statistical significance: ***P < 0.001 versus Ctrl.

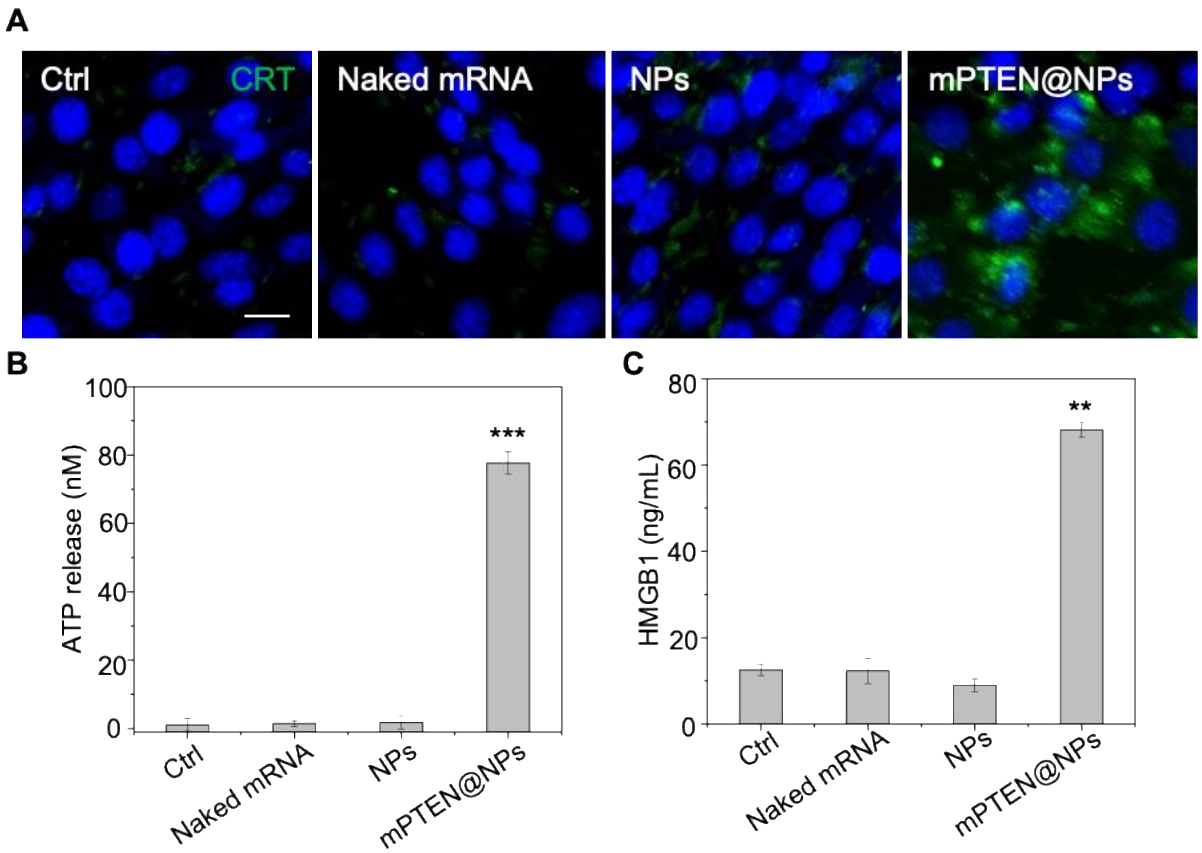

Fig. S19. Analysis of immunogenic cell death markers in BMPC tumor cells. BMPC tumor cells were treated with PBS (Ctrl), naked mRNA, NPs and mPTEN@NPs for 48 hours. Then the cell samples were stained with CRT antibody, and the cell culture medium was collected and measured with ELISA kits according to the manufacturer's instructions. (**A**) CRT expression (green) on plasma membrane, (**B**) ATP release, and (**C**) HMGB1 release were evaluated in vitro. Data are presented as mean ± SD (n = 3 replicates

per group), and analyzed by a one-way ANOVA with a Tukey post-hoc test. **P < 0.01, ***P < 0.001 versus Ctrl. Scale bar, 20 μm.

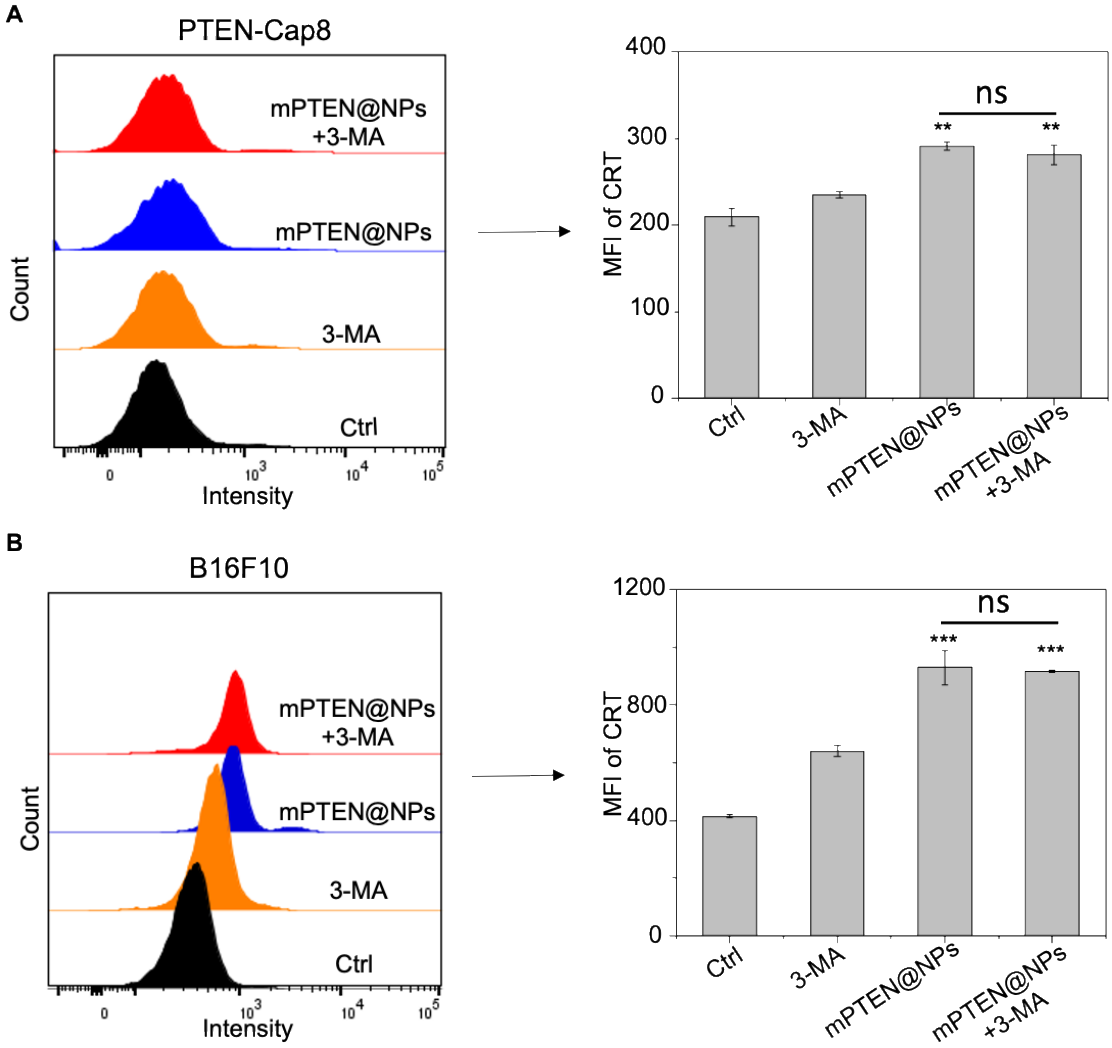

Fig. S20. 3-MA treatment reduces CRT on the surface of tumor cells following mPTEN@NP exposure. (**A**) PTEN-Cap8 and (**B**) B16F10 cells were collected and stained with Alexa Fluor 488-labled CRT antibody after treatment with PBS (Ctrl), 3-MA, mPTEN@NPs, or mPTEN@NPs plus 3-MA for 48 hours. Data are presented as mean ± SD (n = 3 replicates per group), and analyzed by a one-way ANOVA with a Tukey post-hoc test. Statistical significance: **P < 0.01, ***P < 0.001 versus Ctrl; $^{\#}$P < 0.05, $^{\#\#}$P < 0.01. MFI: mean fluorescent intensity.

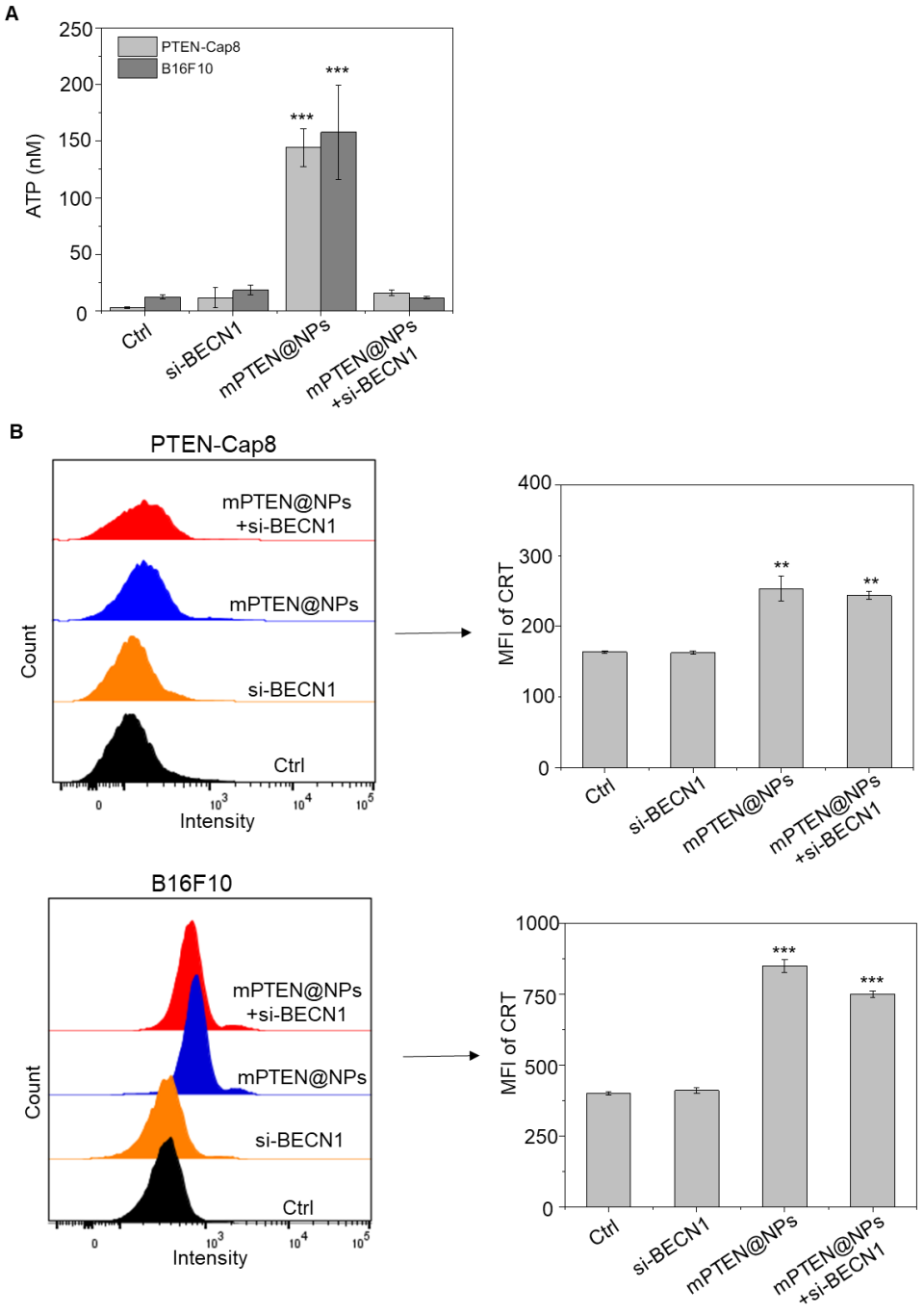

Fig. S21. Effect of autophagy inhibition by RNAi-mediated BECN1 silencing on immunogenic cell death induction by mPTEN@NPs. (**A**) ATP release by indicated tumor cell lines following mPTEN@NP treatment for 48 hours with or without silencing of BECN1 was quantified. (**B**) CRT abundance on the surface of tumor cells following treatment with mPTEN@NPs and silencing of BECN1 was evaluated. The cells were collected and stained with Alexa Fluor 488-labeled CRT antibody after treatment with PBS (Ctrl), si-BECN1, mPTEN@NPs, or mPTEN@NPs + si-BECN1 for 48 hours. Data are presented as mean ± SD (n = 3 replicates per group), and analyzed by a one-way ANOVA with a Tukey post-hoc test. Statistical significance, **P < 0.01, ***P < 0.001 versus Ctrl; $^{\#}$P < 0.05, $^{\#\#}$P < 0.01. MFI: mean fluorescent intensity.

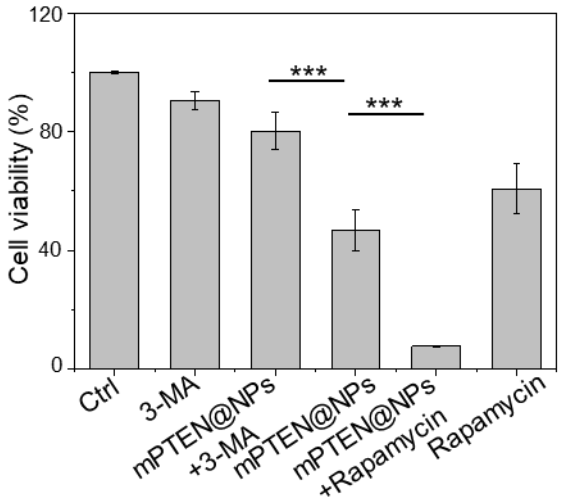

Fig. S22. Effect of autophagy induction or inhibition on the viability of PTEN-Cap8 cells induction by mPTEN@NPs. Autophagy was induced with rapamycin or inhibited with 3-MA treatment in vitro. The cells were measured by AlamarBlue assay after treatment with PBS (Ctrl), si-BECN1, mPTEN@NPs, or mPTEN@NPs + si-BECN1 for 48 hours. Data are presented as mean ± SD (n = 3 replicates per group), and analyzed by a one-way ANOVA with Tukey post-hoc test. Statistical significance: ***P < 0.001.

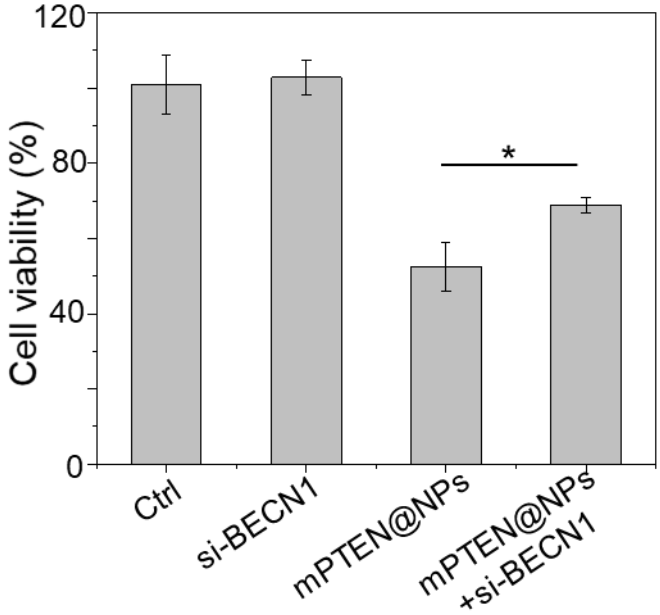

Fig. S23. Effect of autophagy inhibition by RNAi-mediated BECN1 silencing on the viability of PTEN-Cap8 cells co-treated with mPTEN@NPs. PTEN-Cap8 cells were treated with mPTEN@NPs for 48 hours, and BECN1 was silenced in tumor cells. Data are presented as mean ± SD (n = 3 replicates per group) and analyzed by a one-way ANOVA with Tukey post-hoc test. Statistical significance: *P < 0.05.

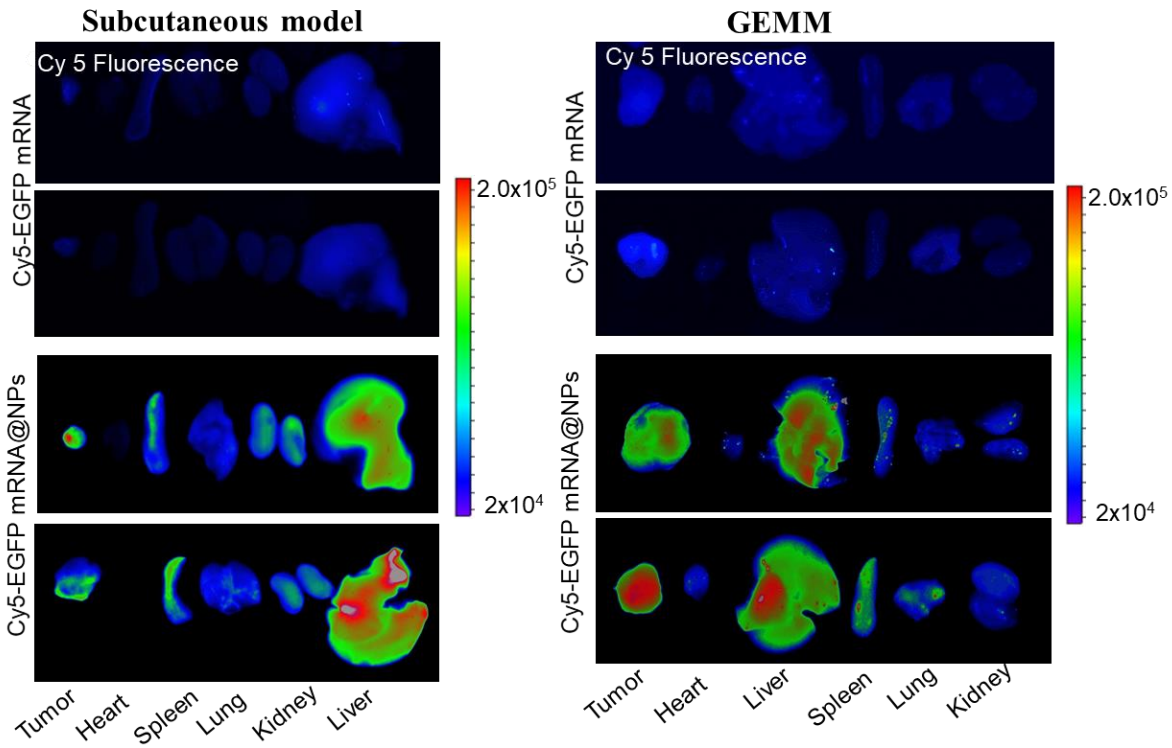

Fig. S24. Biodistribution of Cy5-EGFP mRNA@NPs versus free Cy5-EGFP mRNA in a subcutaneous model of melanoma and genetically engineered mouse model (GEMM) of prostate cancer at 24 hours after intravenous injection.

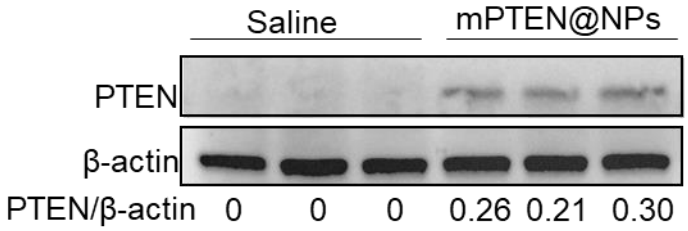

Fig. S25. Western blot analysis for PTEN expression after mPTEN@NPs treatment in the GEMM of *Pten*-null prostate cancer. The tumor tissues (n=3) were collected 48 hours post treatment with mPTEN@NPs. The bottom showed the quantitative analysis results for PTEN expression that were calculated by normalizing PTEN protein band intensity at each condition to that of β-actin.

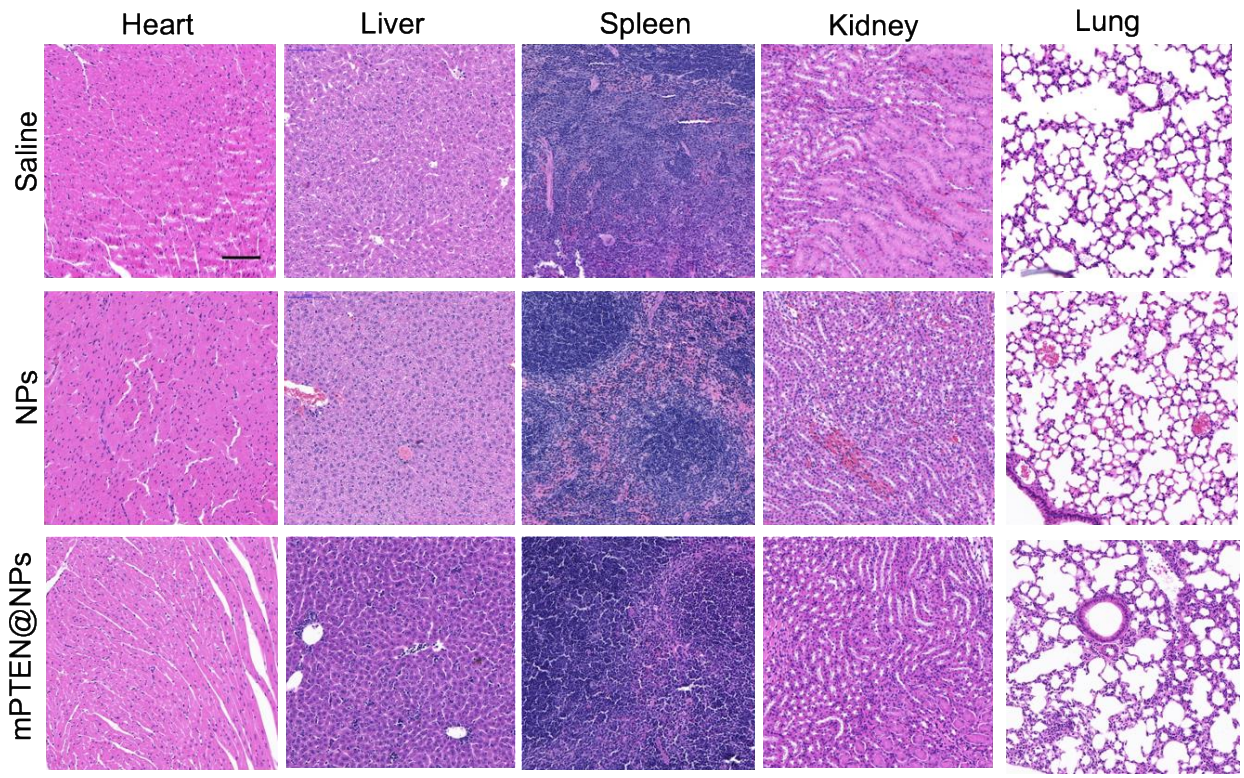

Fig. S26. H&E staining images of the heart, liver, spleen, kidney, and lung tissues. The organs were collected 48 hours post treatment with saline (Ctrl), NPs, and mPTEN@NPs. Scale bar, 100 μm.

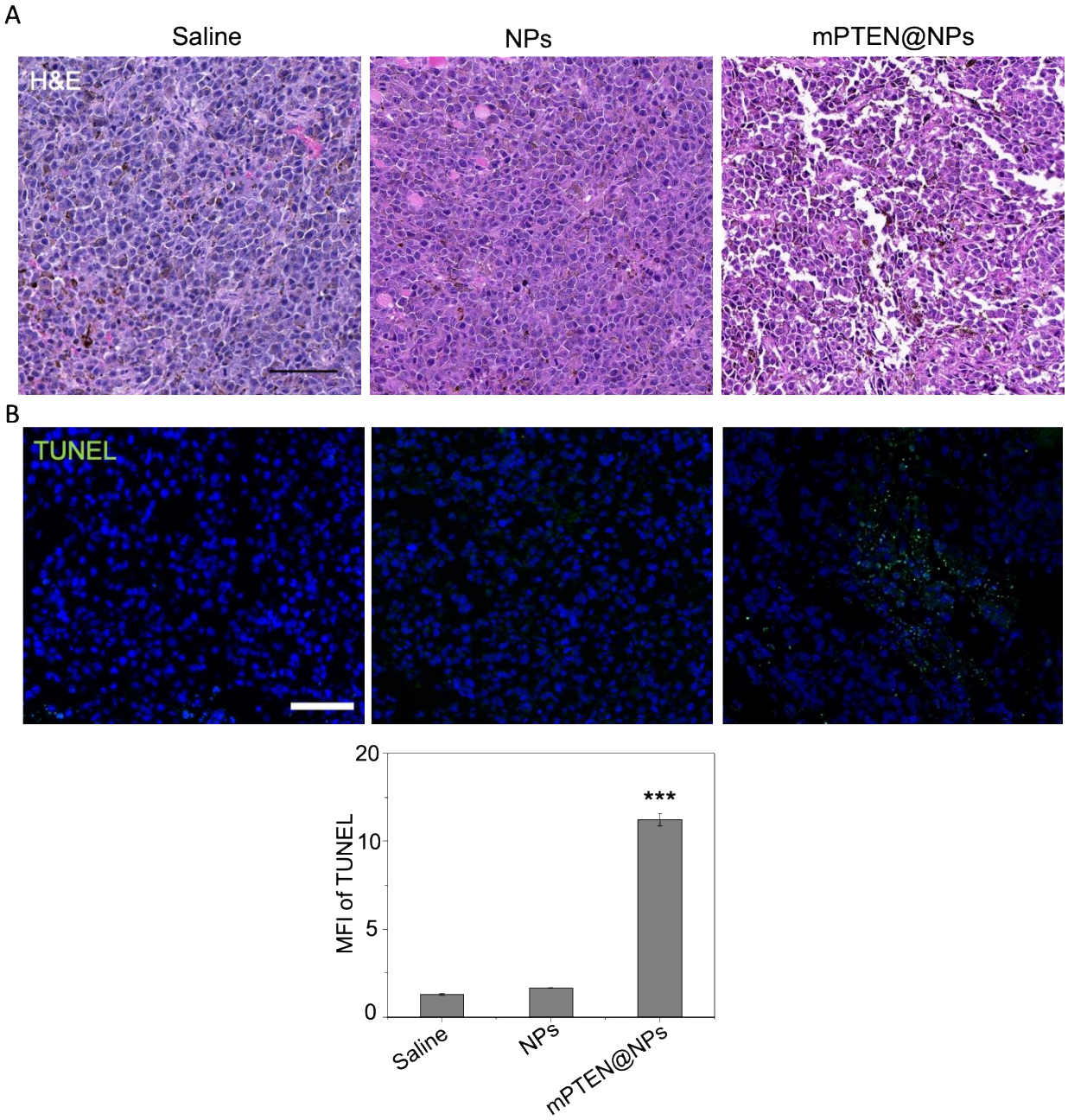

Fig. S27. H&E and TUNEL staining images of tumor tissues. B16F10 tumor tissues were collected 48 hours post the third round of treatment with saline (Ctrl), NPs, or mPTEN@NPs. (**A**) H&E and (**B**) TUNEL staining and quantification of TUNEL staining. Data are presented as mean ± SD (n = 3 mice per group) and analyzed by a one-way ANOVA with Tukey post-hoc test. Statistical significance: ***P < 0.001 versus Ctrl. Scale bar, 50 μm.

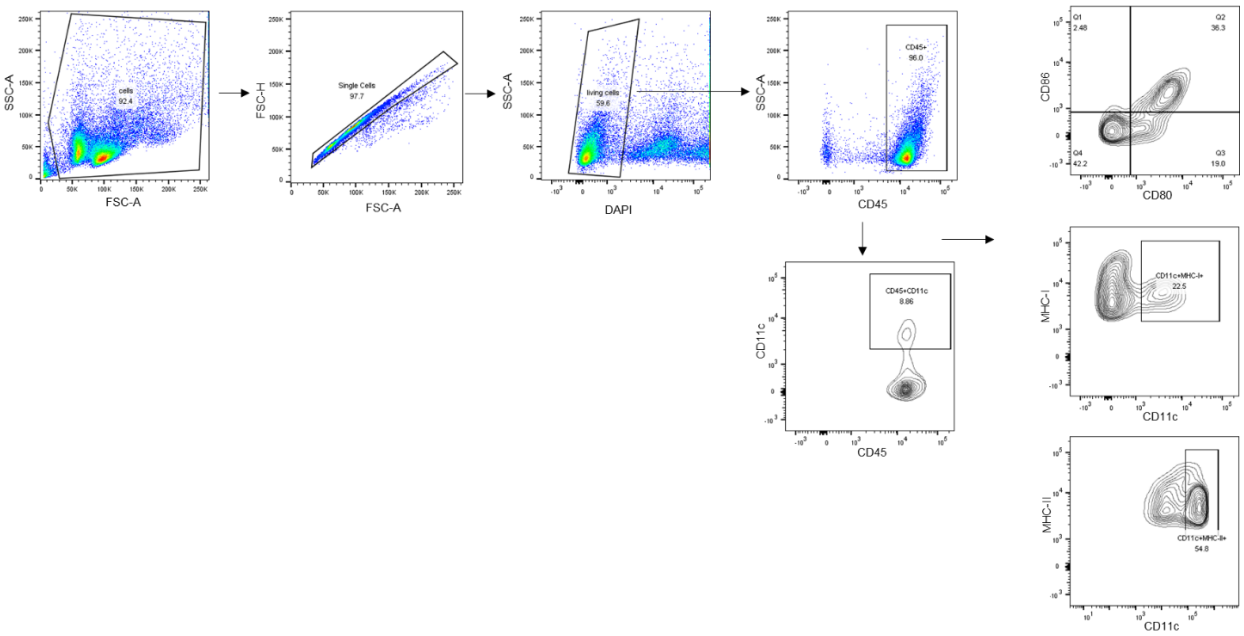

Fig. S28. Primary gating strategy for dendritic cell analysis. Singlet cells were selected from the cell population and dead cells were excluded. $CD11c^{+}CD45^{+}$ dendritic cells were selected from the live cell population. Subsequently, $CD80^{+}CD86^{+}$, $CD11c^{+}$MHC-I^{+} and $CD11c^{+}$MHC-II^{+} cells were analyzed. MHC, major histocompatibility complex; FSC-H, forward scatter height; FSC-A, forward scatter area; SSC-H, side scatter height; SSC-A, side scatter area.

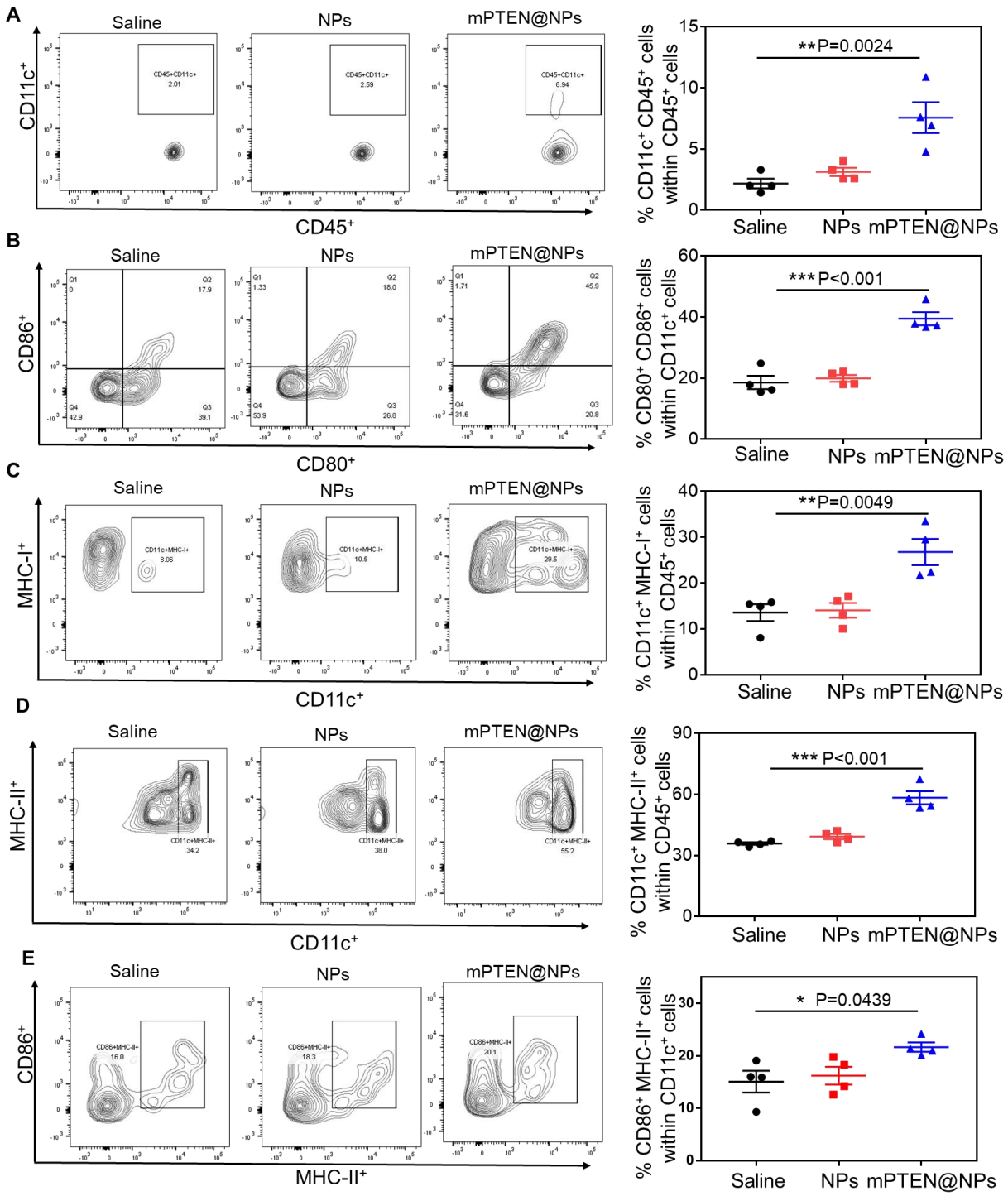

Fig. S29. Representative flow cytometric analysis and quantitation of dendritic cells within lymph node. B16F10 tumor-bearing mice were euthanized and inguinal lymph nodes were isolated 48 hours post the third round of treatment. (**A**) Percentage of $CD11c^+CD45^+$ cells. (**B**) Percentage of $CD80^+CD86^+$ cells. (**C**) Percentage of $CD11c^+MHC\text{-}I^+$ cells. (**D**) Percentage of $CD11c^+MHC\text{-}II^+$ cells. (**E**) Percentage of $CD86^+MHC\text{-}II^+$ cells. Data are presented as mean ± SEM (n = 4 mice per group). Statistical significance was calculated by a one-way ANOVA with a Tukey post-hoc test. **P < 0.01, ***P < 0.001.

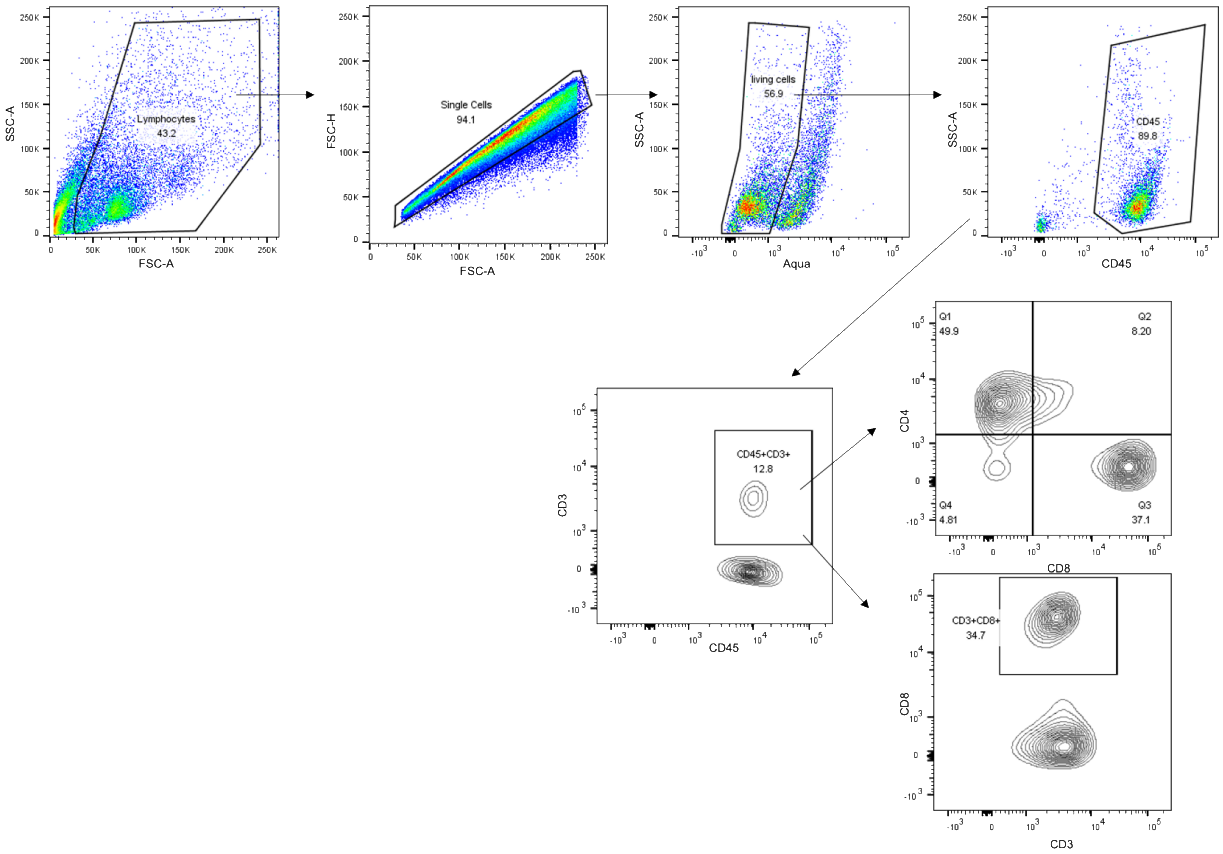

Fig. S30. Primary gating strategy for analysis of T cells in tumors. B16F10 tumor-bearing mice were euthanized and tumors were isolated 48 hours post the third round of treatment. Singlet cells were selected from the cell population and dead cells were excluded. For T cells, $CD3^{+}CD45^{+}$ T cells were selected from the live cell population. Subsequently, $CD8^{+}CD3^{+}$ and $CD4^{+}CD3^{+}$ T cells were selected from the T cell population. Finally, IFN-$\gamma^{+}CD8^{+}$, T-$bet^{+}CD8^{+}$, IFN-$\gamma^{+}CD4^{+}$ and $Foxp3^{+}CD25^{+}CD4^{+}$ T cells were analyzed. T-bet, T-box expressed in T cells; IFN, interferon.

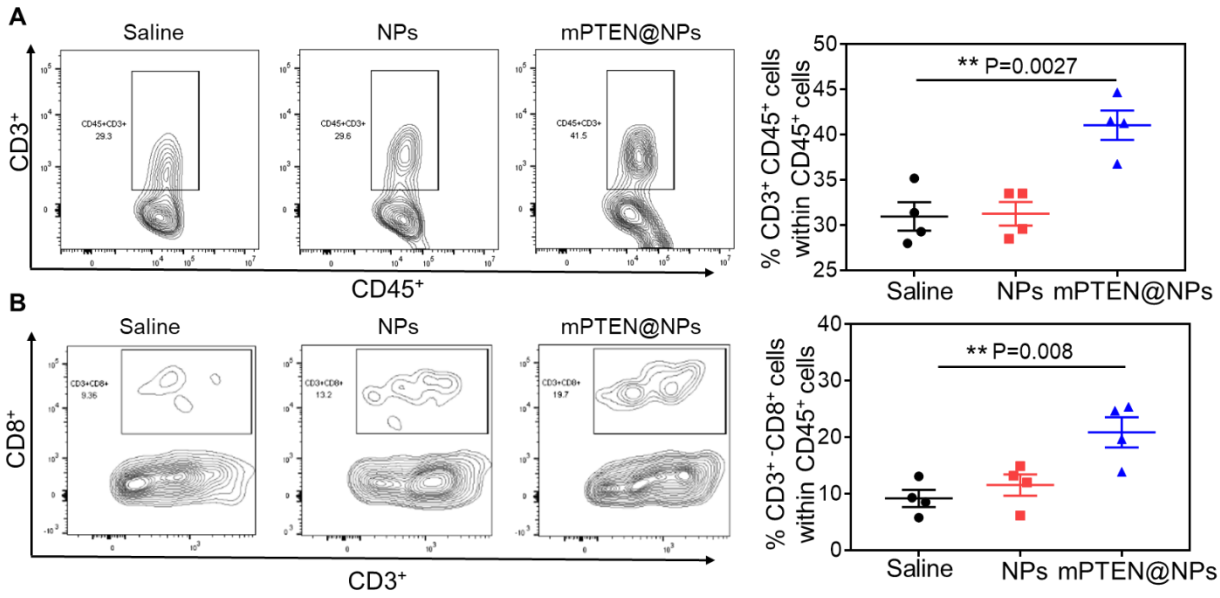

Fig. S31. **Representative flow cytometric analysis and quantification for the percent of CD3$^+$ or CD8$^+$ T cells within the tumor.** B16F10 tumor-bearing mice were euthanized and tumors were isolated 48 hours post the third round of treatment. (**A**) Percentage of CD3$^+$CD45$^+$ cells. (**B**) Percentage of CD8$^+$CD3$^+$ cells. Data are presented as mean ± SEM (n = 4 mice per group). Statistical significance was calculated by a one-way ANOVA with a Tukey post-hoc test. **P < 0.01.

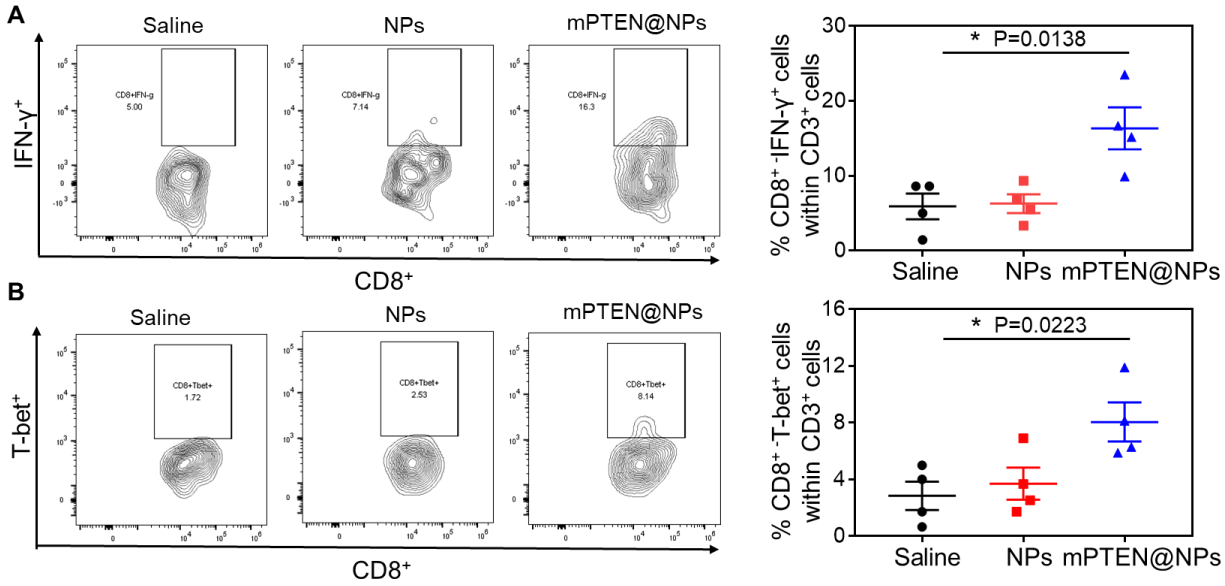

Fig. S32. **Representative flow cytometric analysis and the quantitative results of CD8$^+$ effector T cells in the tumor.** B16F10 tumor-bearing mice were euthanized and tumors were isolated 48 hours post the third round of treatment. (**A**) Percentage of IFN-γ$^+$CD8$^+$ T cells. (**B**) Percentage of T-bet$^+$CD8$^+$ T cells. Data are presented as mean ± SEM (n = 4 mice per group). Statistical significance was calculated by a one-way ANOVA with a Tukey post-hoc test. *P < 0.05.

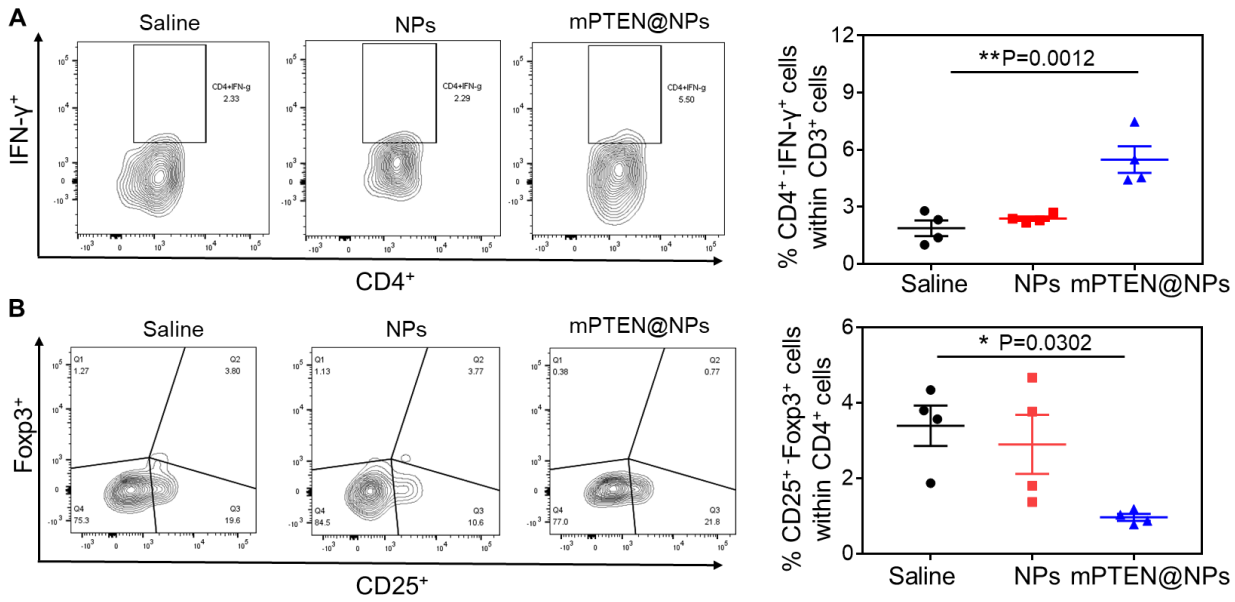

Fig. S33. **Representative flow cytometric analysis and the quantitative results of T_{h1} and T_{reg} cells in the tumor.** B16F10 tumor-bearing mice were euthanized and tumors were isolated 48 hours post the third round of treatment. (**A**) Percentage of IFN-γ^+CD4$^+$ T cells. (**B**) Percentage of Foxp3$^+$CD25$^+$ CD4$^+$ T cells. Data are presented as mean ± SEM (n = 4 mice per group). Statistical significance was calculated by a one-way ANOVA with a Tukey post-hoc test. *P < 0.05, **P < 0.01.

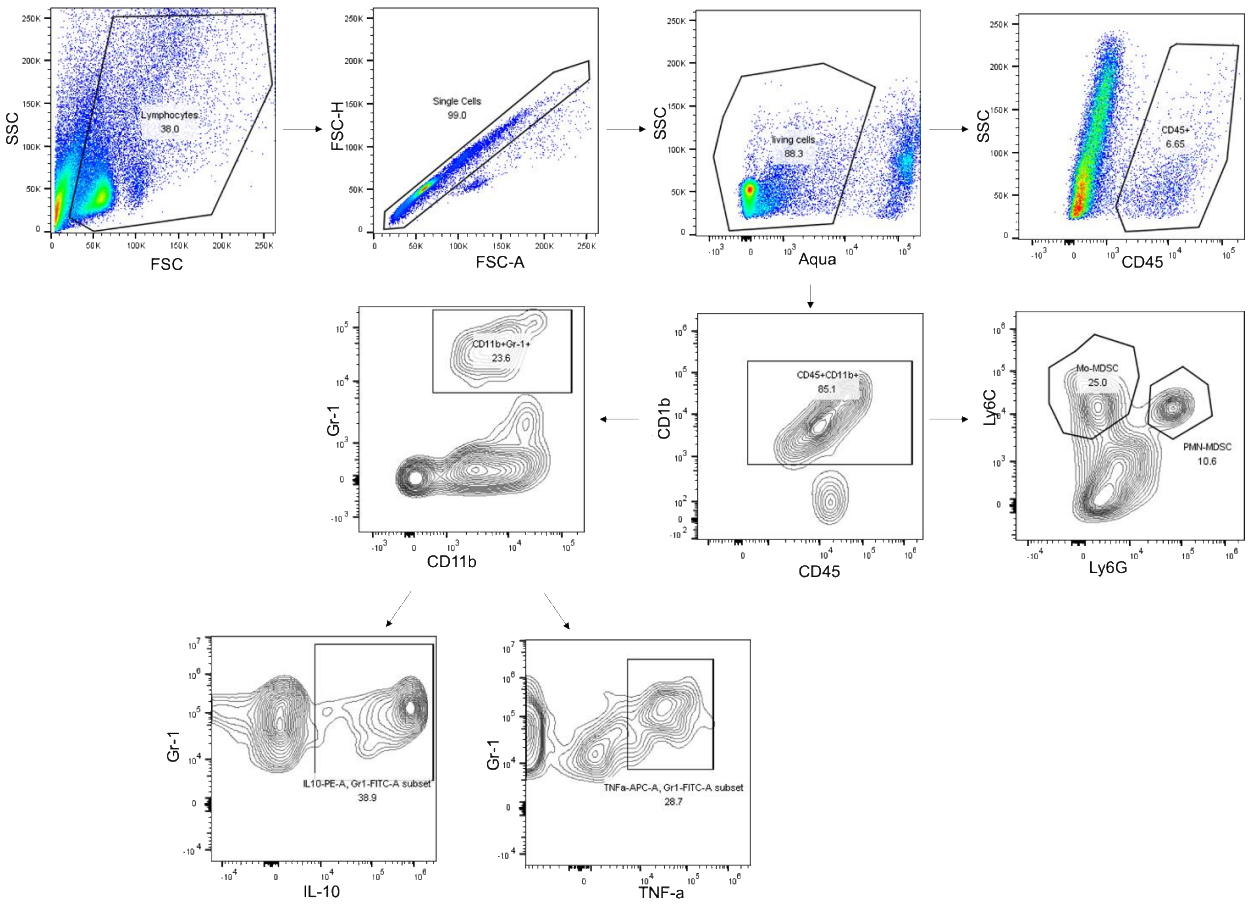

Fig. S34. Primary gating strategy for analysis of myeloid-derived suppressor cells in tumors. B16F10 tumor-bearing mice were euthanized and tumors were isolated 48 hours post the third round of treatment. Singlet cells were selected from the cell population and dead cells were excluded. For myeloid-derived suppressor cells, $CD11b^{+}CD45^{+}$ cells were selected from the live cell population. Subsequently, $CD11b^{+}Gr\text{-}1^{+}$ myeloid-derived suppressor cells, monocytic myeloid-derived suppressor cells ($Ly6G^{-}Ly6C^{+}$) and polymorphonuclear myeloid-derived suppressor cells ($Ly6G^{+}Ly6C^{+}$) were analyzed. Finally, IL-10 and TNF-α myeloid-derived suppressor cells were analyzed.

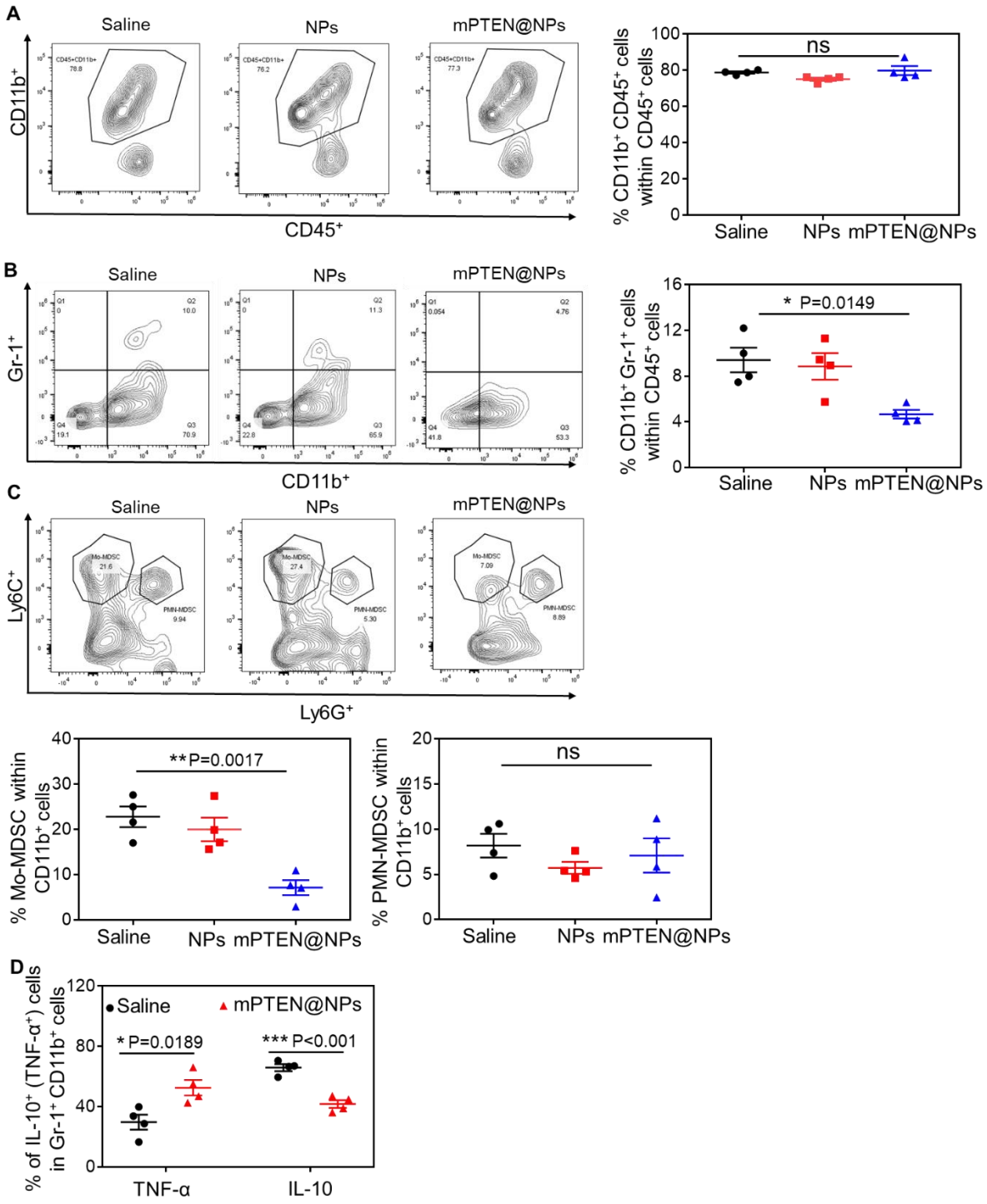

Fig. S35. Representative flow cytometric analysis and the quantitative results of myeloid-derived suppressor cells in the tumor. B16F10 tumor-bearing mice were euthanized and tumors were isolated 48 hours post the third round of treatment. (**A**) Percentage of $CD11b^{+}CD45^{+}$ cells. (**B**) Percentage of $CD11b^{+}Gr\text{-}1^{+}$ cells. (**C**) Percentage of monocytic myeloid-derived suppressor cells and polymorphonuclear myeloid-derived suppressor cells. (**D**) Production of TNF-α or IL-10 by myeloid-derived suppressor cells was quantified by intracellular cytokine staining in saline- or mPTEN@NPs-treated mice. Data are presented as mean ± SEM (n = 4 mice per group). Statistical significance was calculated by a one-way ANOVA with a Tukey post-hoc test. ns: no significance, *P < 0.05, **P < 0.01, ***P < 0.001.

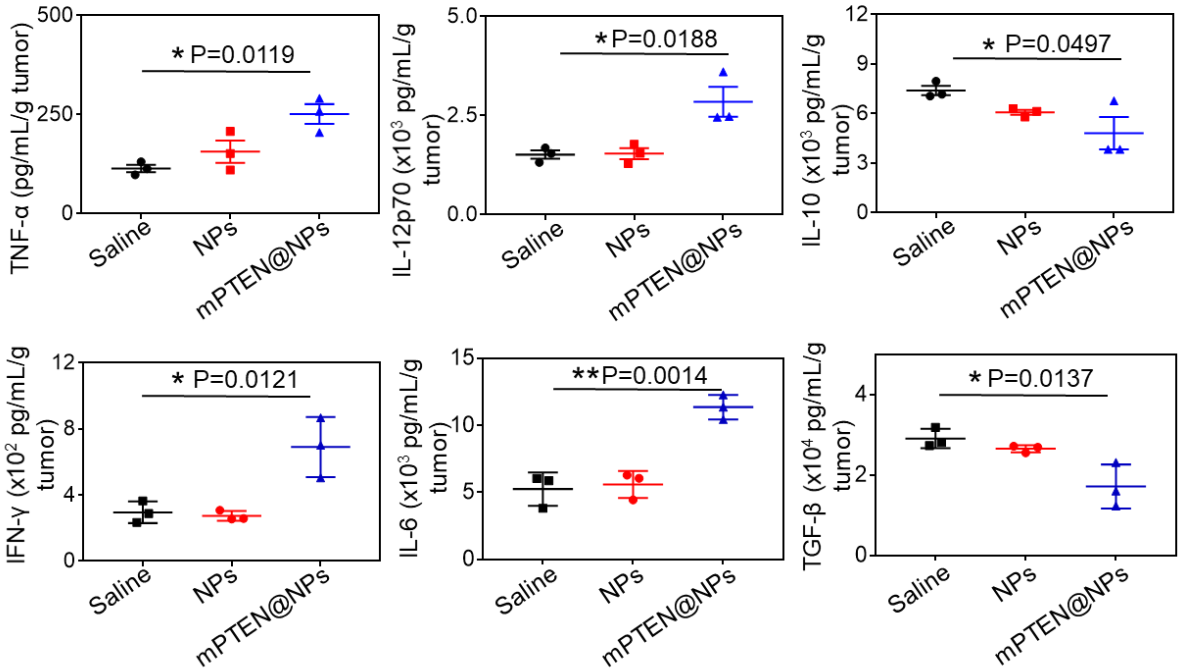

Fig. S36. Cytokine concentrations in the tumor after treatment. B16F10 tumor-bearing mice were euthanized and tumors were isolated 48 hours post the third round of treatment. Data are presented as mean ± SEM (n = 3 mice per group). Statistical significance was calculated by a one-way ANOVA with a Tukey post-hoc test. *P < 0.05, **P < 0.01. IL, interleukin; TNF, tumor necrosis factor; IFN, interferon.

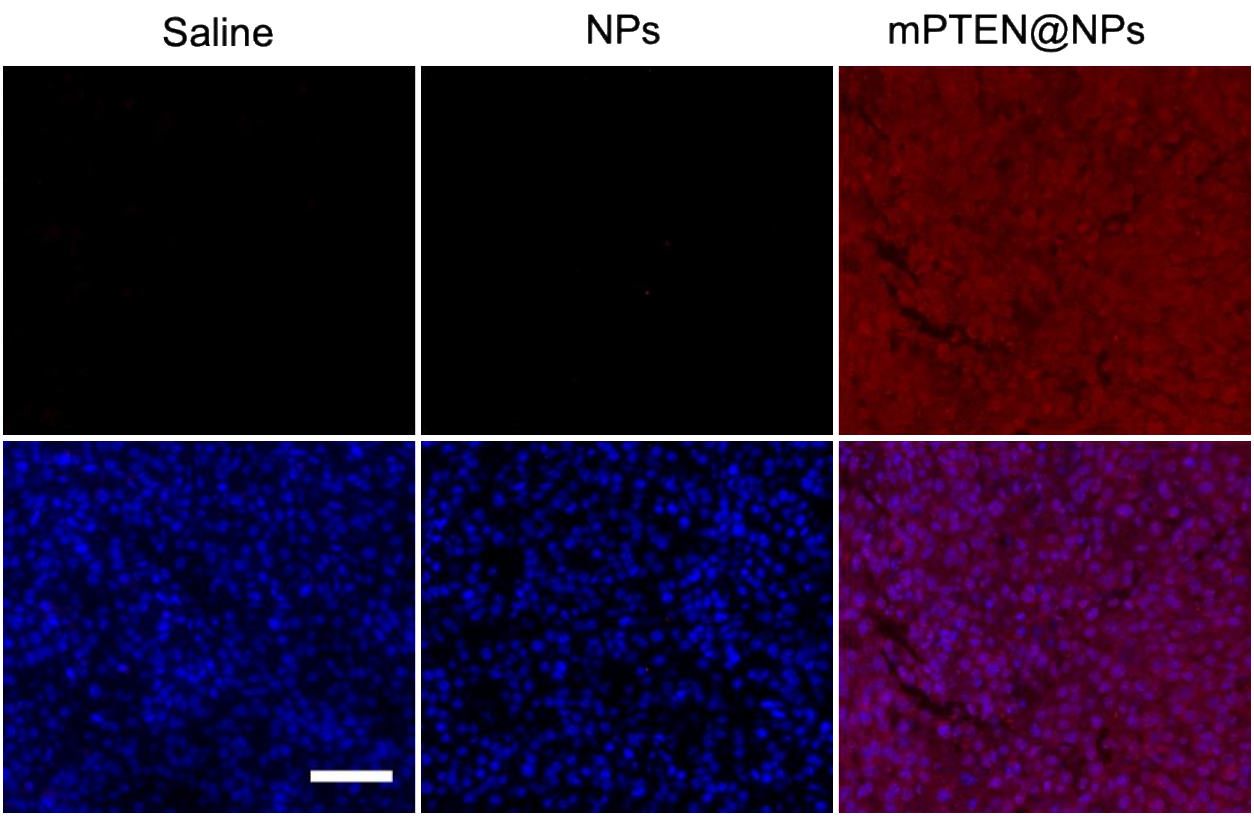

Fig. S37. Immunofluorescence staining of tumor tissues evaluating CRT expression after treatment with saline, control NPs, or mPTEN@NPs. B6F10 tumor-bearing mice were euthanized and tumors were isolated 48 hours post the third round of treatment. CRT staining is shown in red. Scale bar, 50 μm.

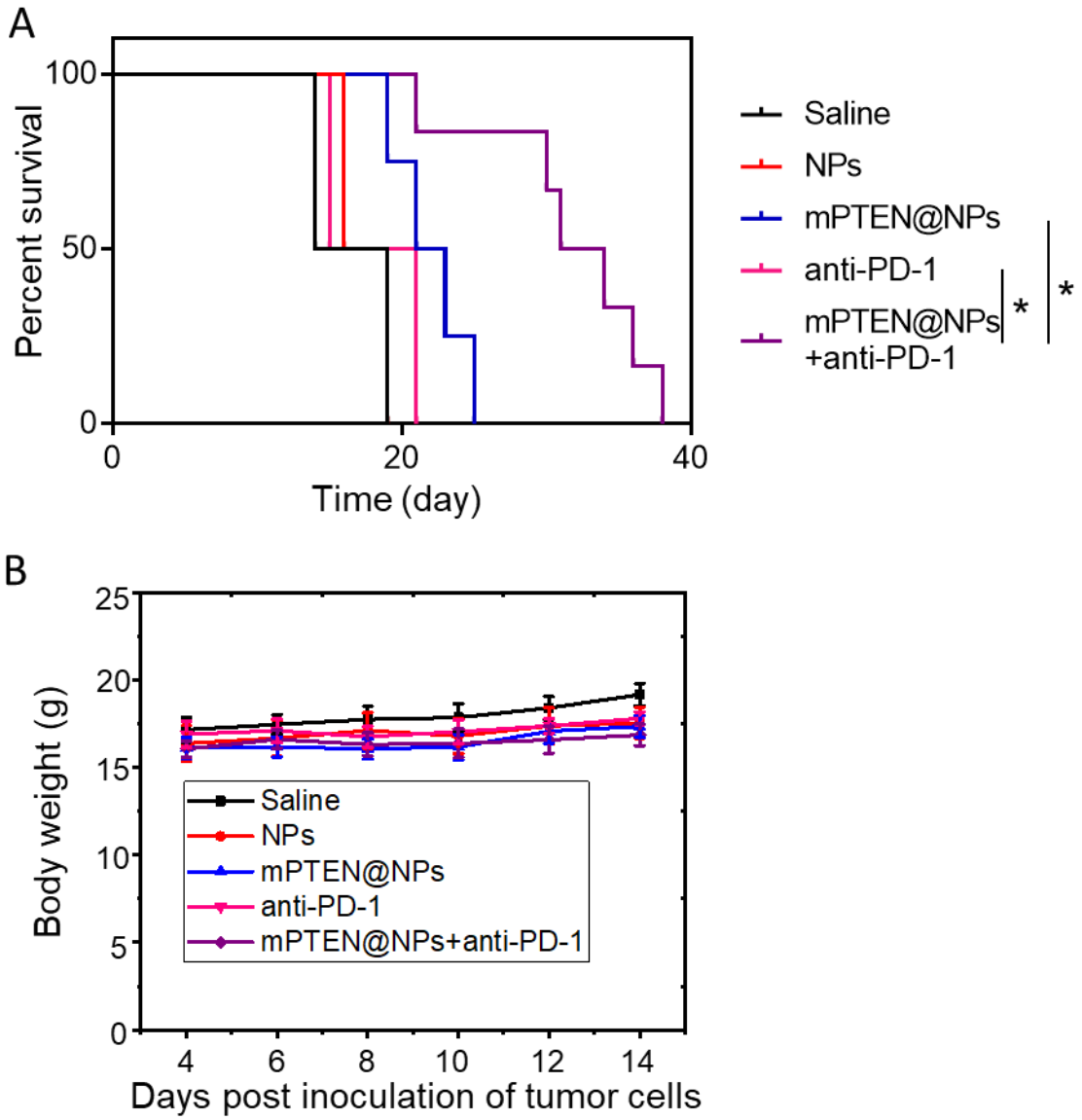

Fig. S38. Evaluation of survival and safety of B16F10 tumor-bearing mice by co-treatment of mPTEN@NPs with anti-PD-1. (**A**) The survival of mice after three rounds of treatment. Log-rank test. *P<0.05, **P<0.01. (**B**) Body weight of mice treated with the indicated formulations.

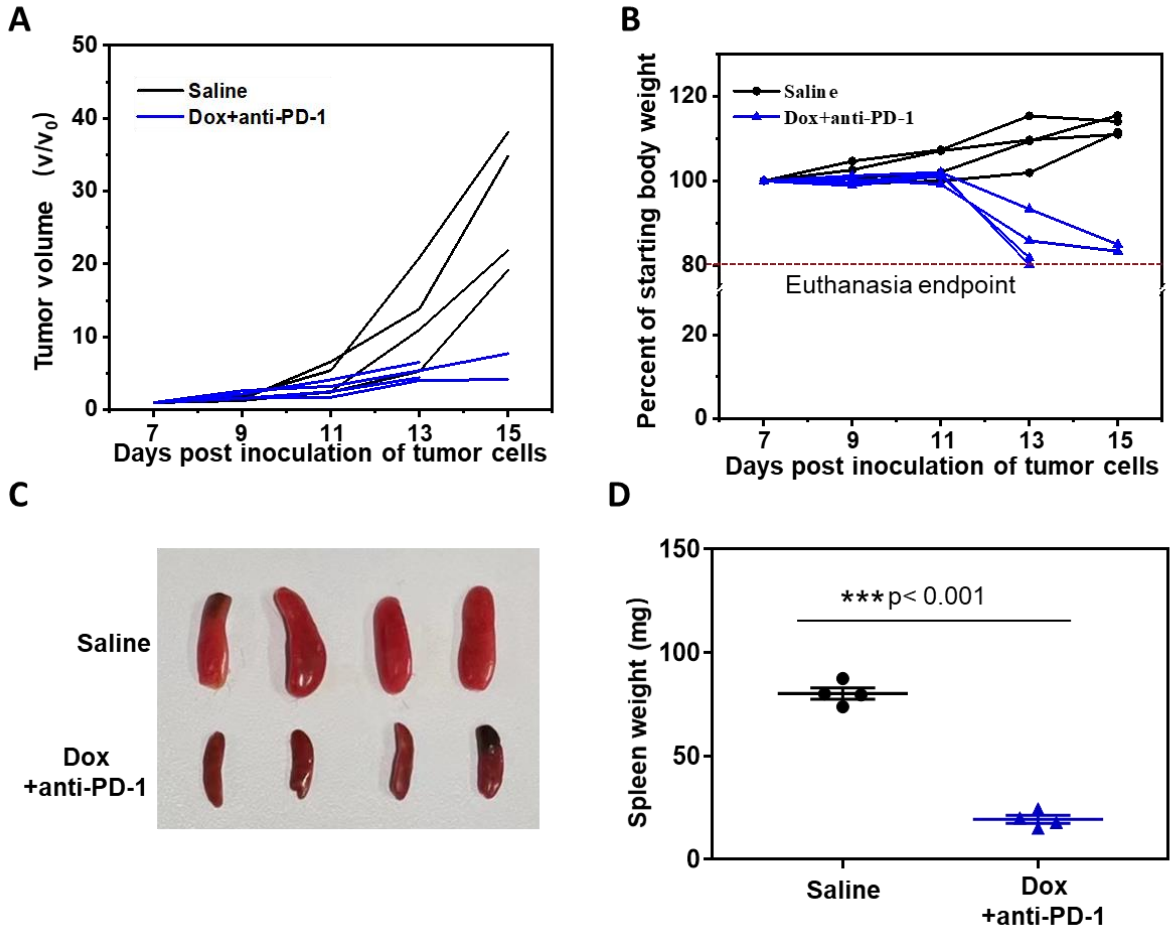

Fig. S39. Evaluation of anti-tumor efficacy and in vivo side effects of co- treatment of doxorubicin (Dox) with anti-PD-1. (**A**) Individual growth curves for B16F10 tumor-bearing mice (n = 4 mice per group) treated with saline or Dox+anti-PD-1 every 3 days for 3 rounds. (**B**) Change in body weight of mice treated with the indicated formulations is shown. Mice were euthanized when weight was 80% of starting body weight. (**C**) Spleen size and (**D**) spleen weight of mice treated with the indicated formulations were measured. Data are represented as mean ± SD (n = 4 mice per group). Statistical significance was calculated by a Student's *t*-test. ***P < 0.001.

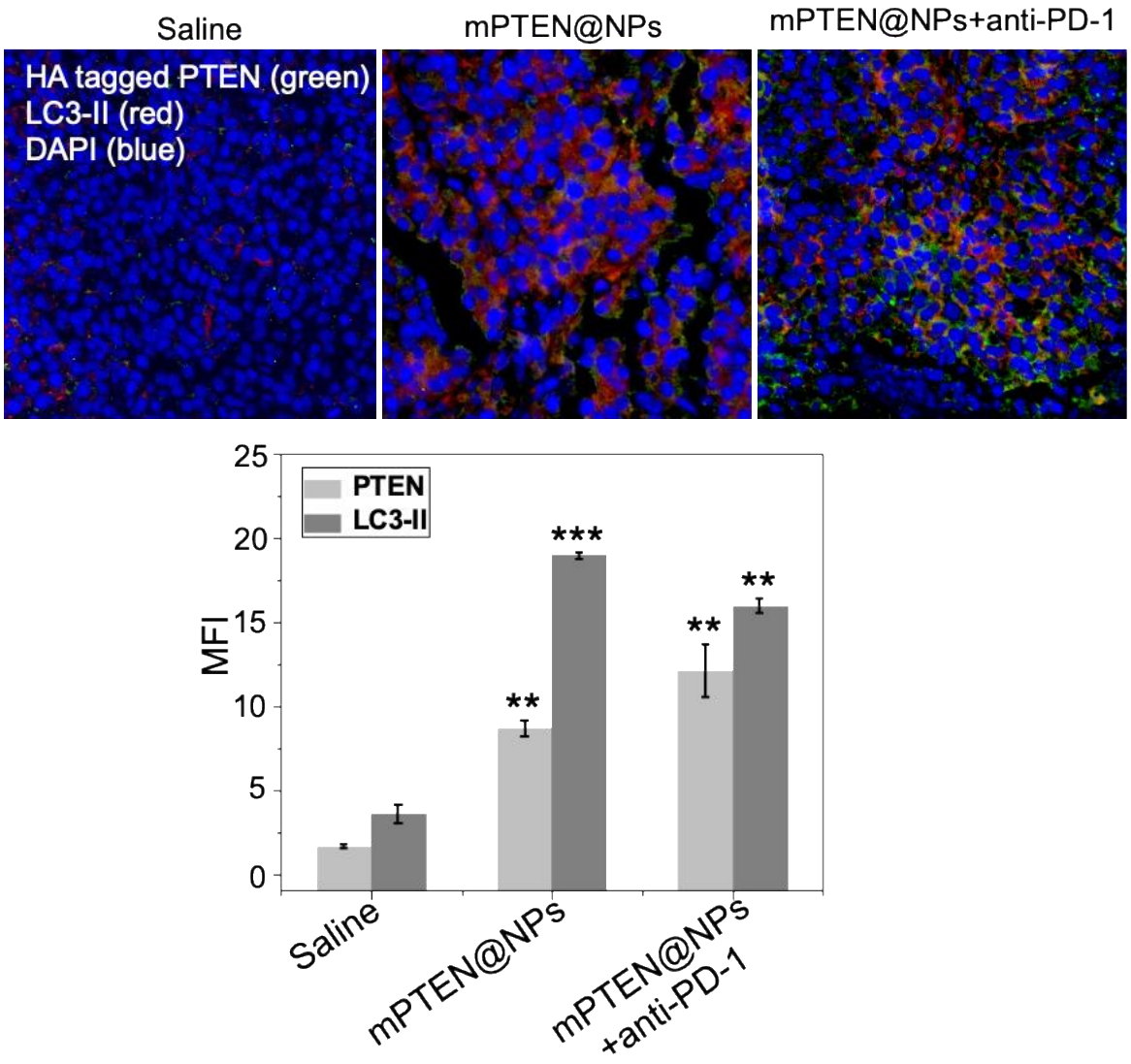

Fig. S40. Immunofluorescence staining of tumor tissues and quantitation of HA-PTEN and LC3-II after treatment with saline (Ctrl), mPTEN@NPs, or mPTEN@NPs plus anti-PD-1. B16F10 tumor-bearing mice were euthanized and tumors were isolated 48 hours post the third round of treatment. Data are presented by mean ± SD (n=3 mice per group). Data were analyzed using a one-way ANOVA with a Tukey post-hoc test. **P < 0.01, ***P < 0.001 versus saline. Scale bar, 50 μm. HA-PTEN, hemagglutinin-tagged PTEN; LC3-II, autophagic marker proteins light chain 3-II; MFI, mean fluorescent intensity.

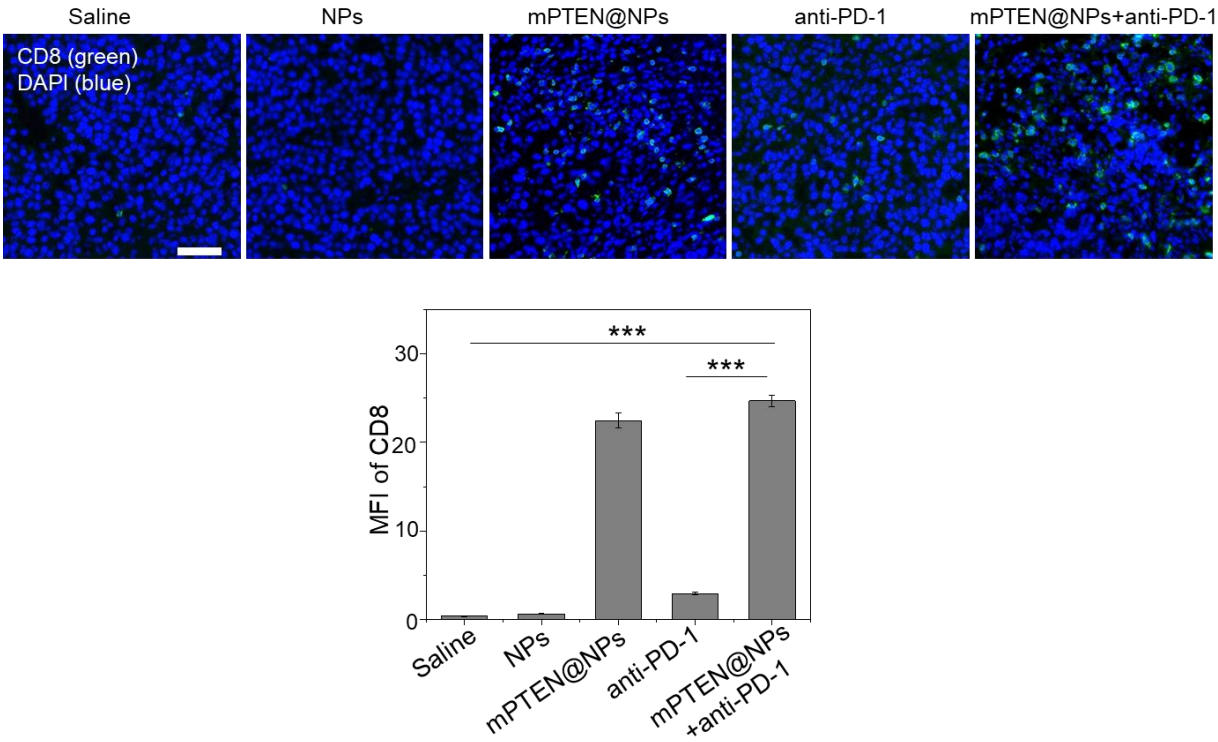

Fig. S41. Immunofluorescence staining of tumor tissues and quantitation of $CD8^+$ T cell infiltration after treatment with saline (Ctrl), NPs, mPTEN@NPs, anti-PD-1, or mPTEN@NPs plus anti-PD-1. B16F10 tumor-bearing mice were euthanized and tumors were isolated 48 hours post the third round of treatment. $CD8^+$ T cells are shown in green. Data are presented by mean ± SD (n = 3 mice per group). Data were analyzed using a one-way ANOVA with a Tukey post-hoc test. ***P < 0.001. Scale bar, 50 μm. MFI: mean fluorescent intensity.

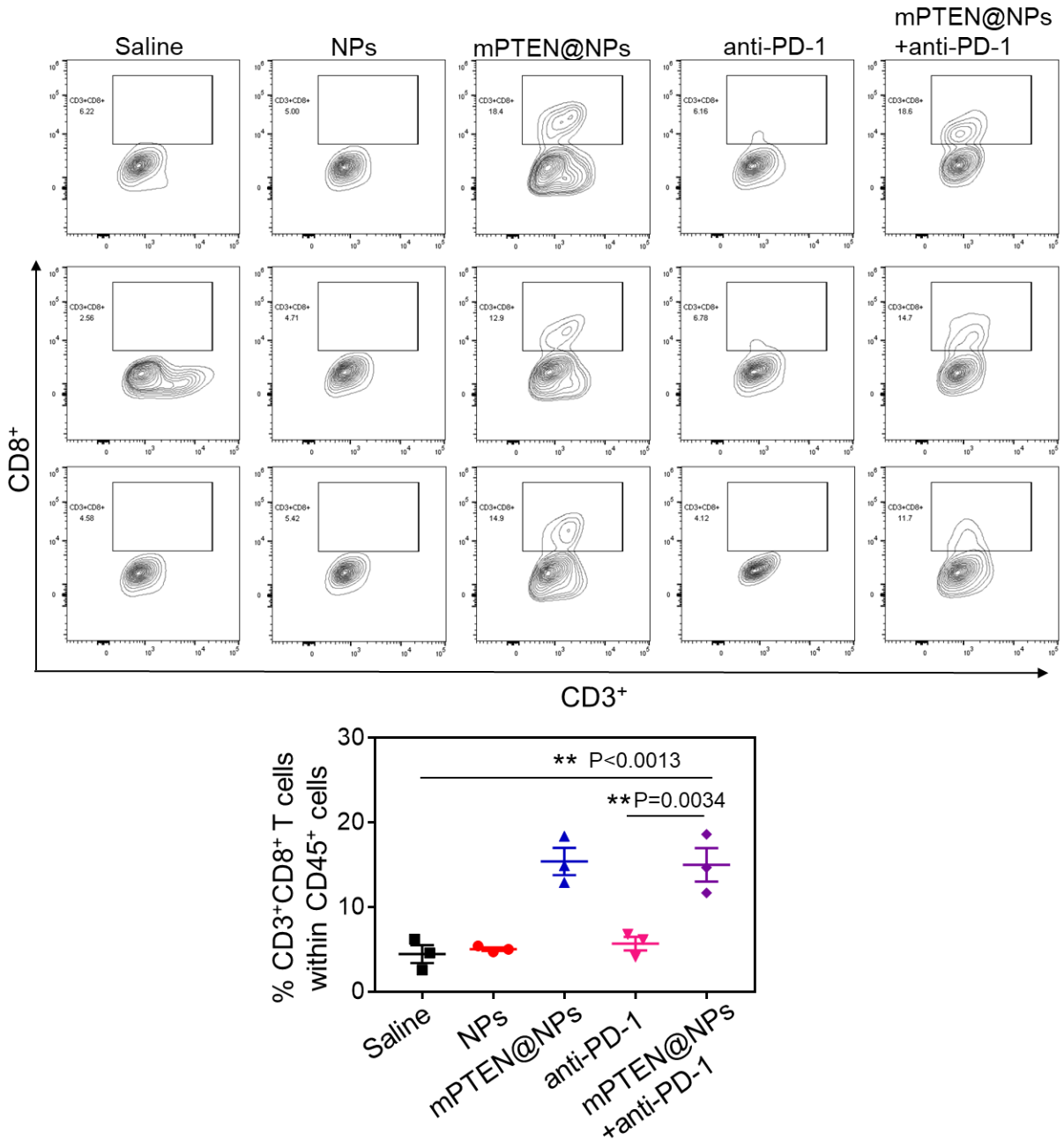

Fig. S42. Representative flow cytometric analysis and quantitation of CD8$^+$ T cells within the tumor. B16F10 tumor-bearing mice were euthanized and tumors were isolated 48 hours post the third round of treatment. Data are presented as mean ± SEM (n = 3 mice per group). Statistical significance was calculated by a one-way ANOVA with a Tukey post-hoc test. **P < 0.01.

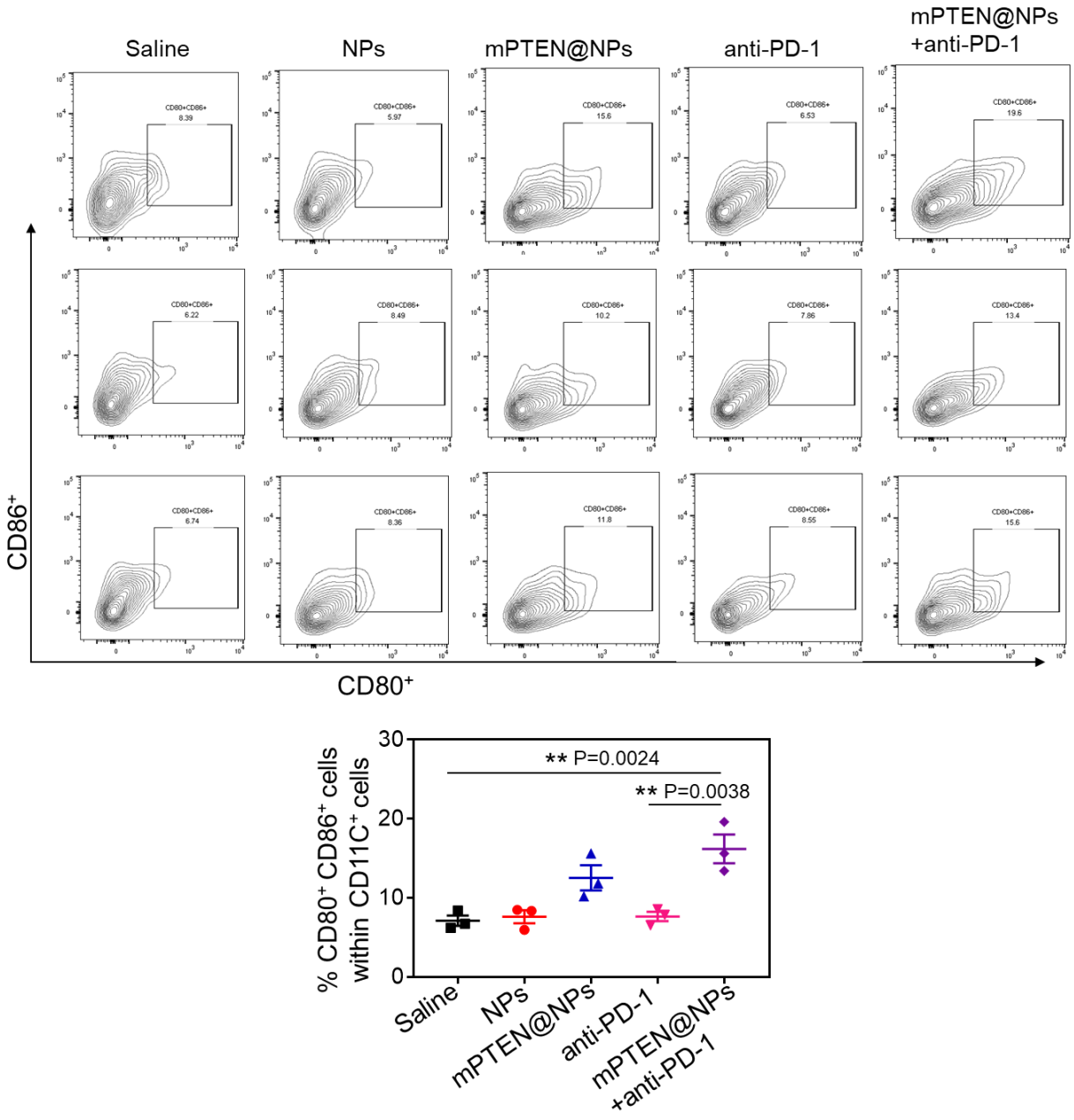

Fig. S43. Representative flow cytometric analysis and quantitation of dendritic cells within the lymph node. B16F10 tumor-bearing mice were euthanized and inguinal lymph node were isolated 48 hours post the third round of treatment. Data are presented as mean ± SEM (n = 3 mice per group). Statistical significance was calculated by a one-way ANOVA with a Tukey post-hoc test. **P < 0.01.

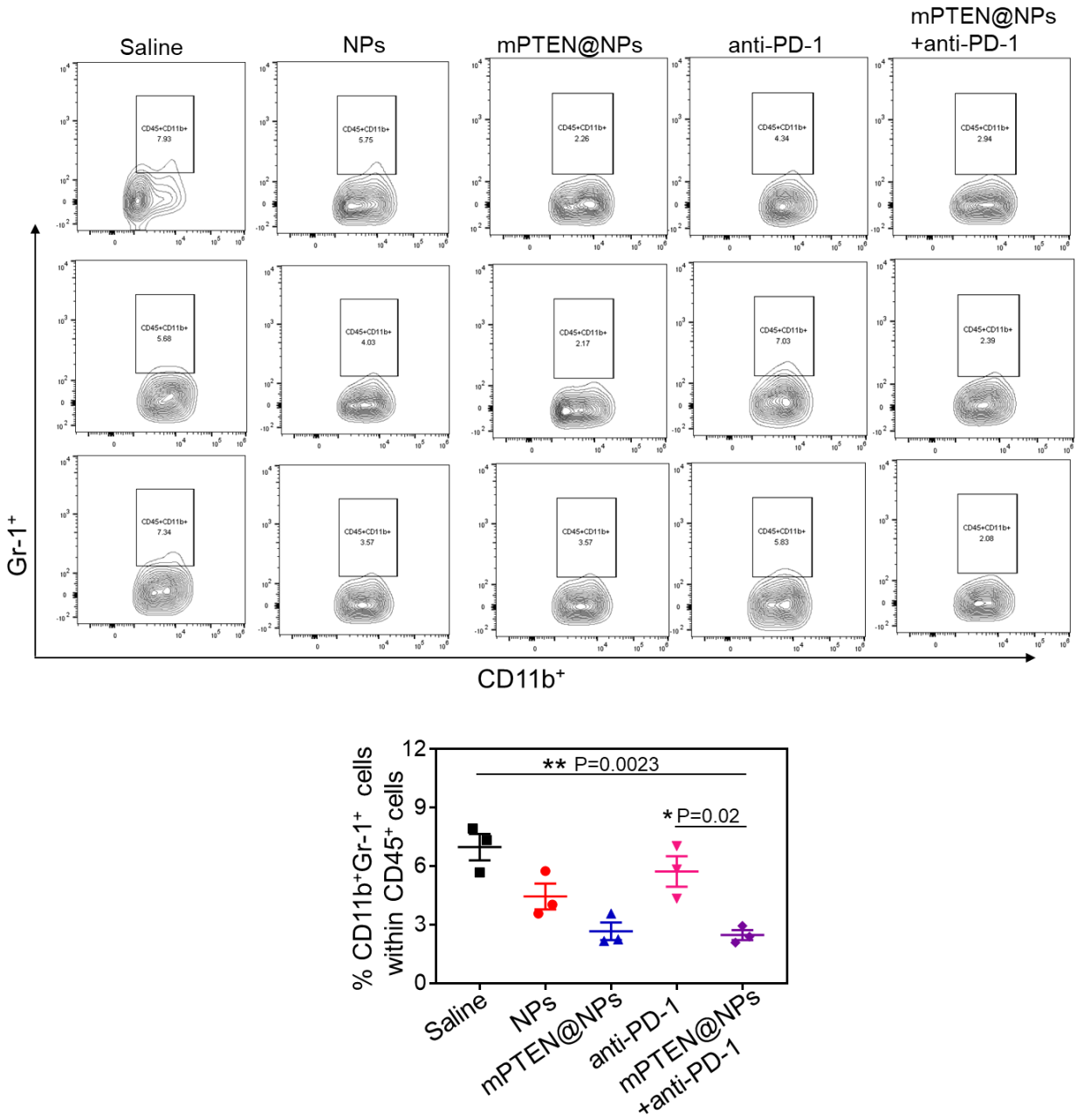

Fig. S44. Representative flow cytometric analysis and quantitation of CD11b$^+$Gr-1 myeloid-derived suppressor cells within the tumor. B16F10 tumor-bearing mice were euthanized and tumor tissues were isolated 48 hours post the third round of treatment. Data are presented as mean ± SEM (n = 3 mice per group). Statistical significance was calculated by a one-way ANOVA with a Tukey post-hoc test. *P < 0.05, **P < 0.01.

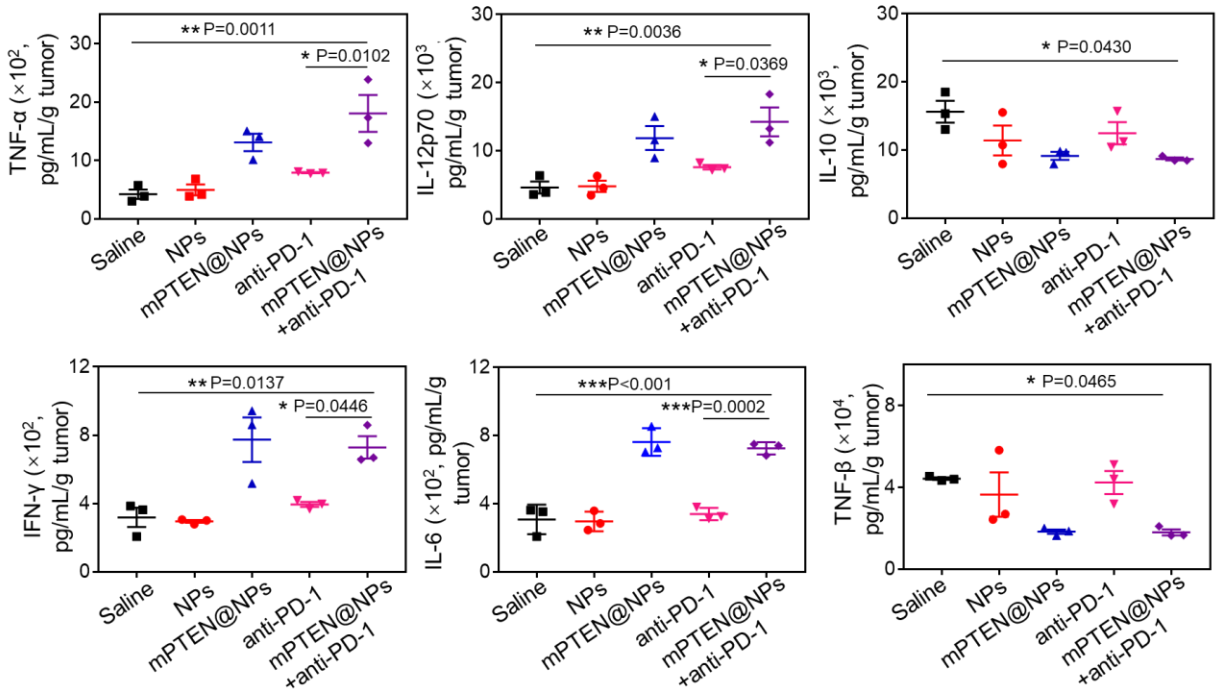

Fig. S45. Cytokine concentrations in the tumor after treatment with saline (Ctrl), NPs, mPTEN@NPs, anti-PD-1, or mPTEN@NPs plus anti-PD-1. B16F10 tumor-bearing mice were euthanized and tumor tissues were isolated 48 hours post the third round of treatment. Data are presented as mean ± SEM (n = 3 mice per group). Statistical significance was calculated by a one-way ANOVA with a Tukey post-hoc test. *P < 0.05, **P < 0.01, ***P < 0.001.

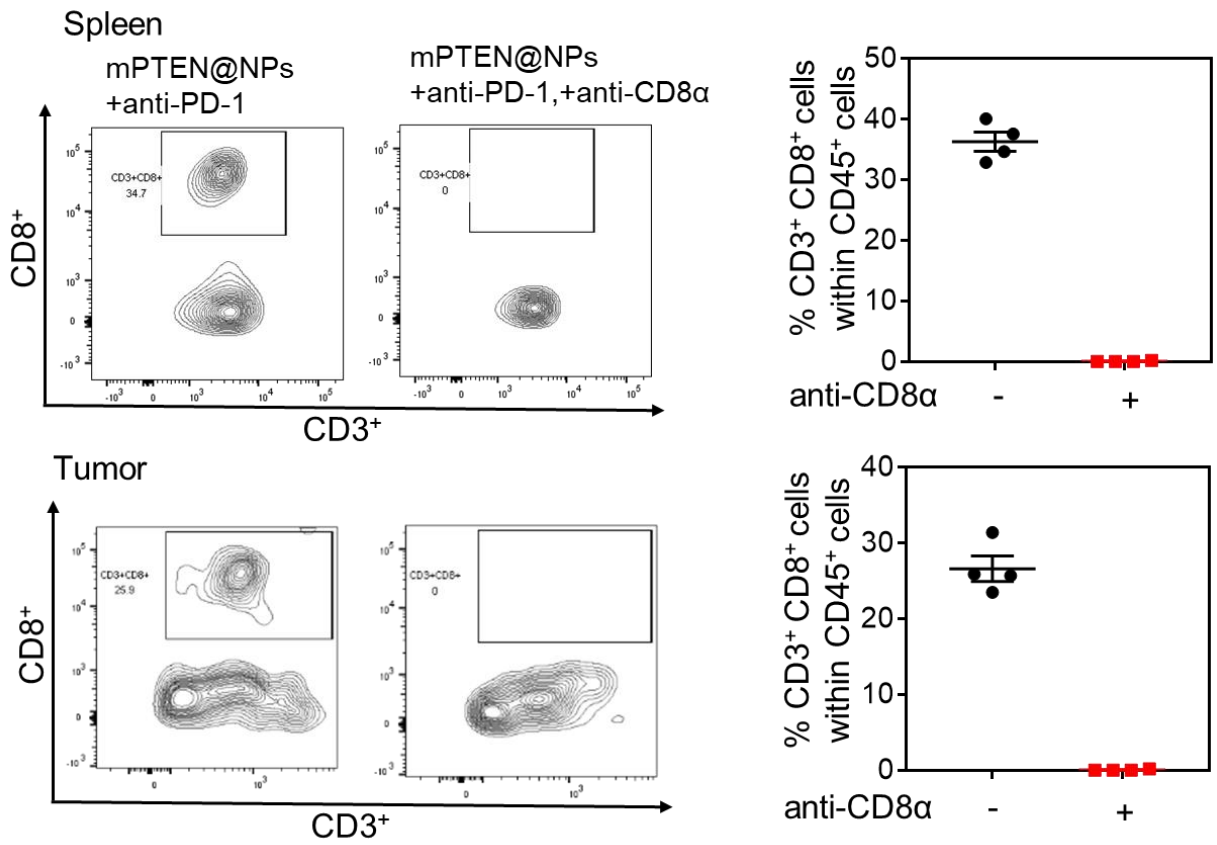

Fig. S46. Representative flow cytometric analysis and quantitation of CD8$^+$ T cells within the spleen or tumor. B16F10 tumor-bearing mice were euthanized and spleen and tumor tissues were isolated 48 hours post third round of treatment. Data are presented as mean ± SEM (n = 4 mice per group).

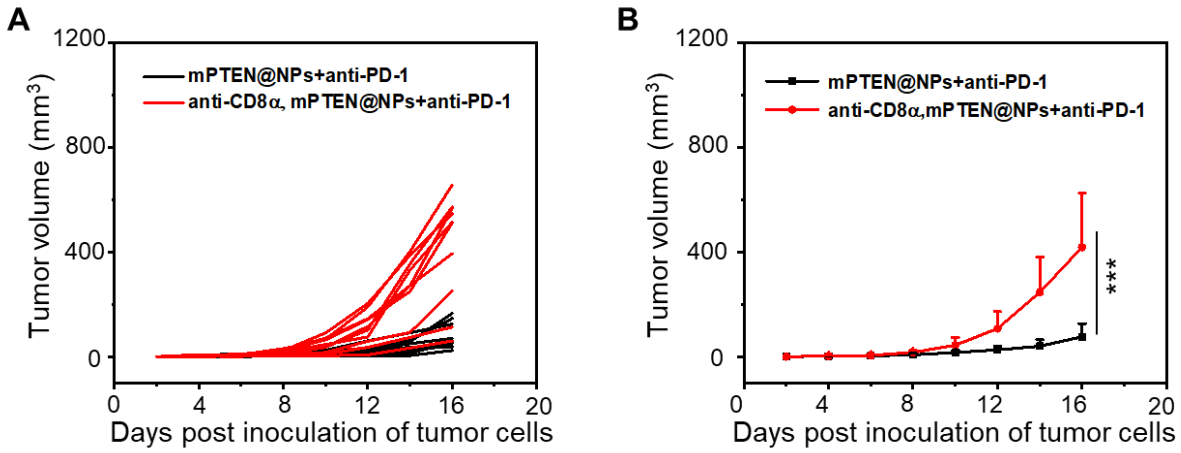

Fig. S47. Depletion of CD8$^+$ T cells reduced anti-tumor efficacy of co-treatment of mPTEN@NPs with anti-PD-1. (**A**) Individual growth curves for B16F10 tumor-bearing mice treated with indicated formulations. (**B**) The average tumor growth curves for B16F10 tumor-bearing mice treated with indicated formulations. Data are represented as mean ± SD (n = 10 mice per group). Statistical significance was calculated by a Mann Whitney test. ***P < 0.001.

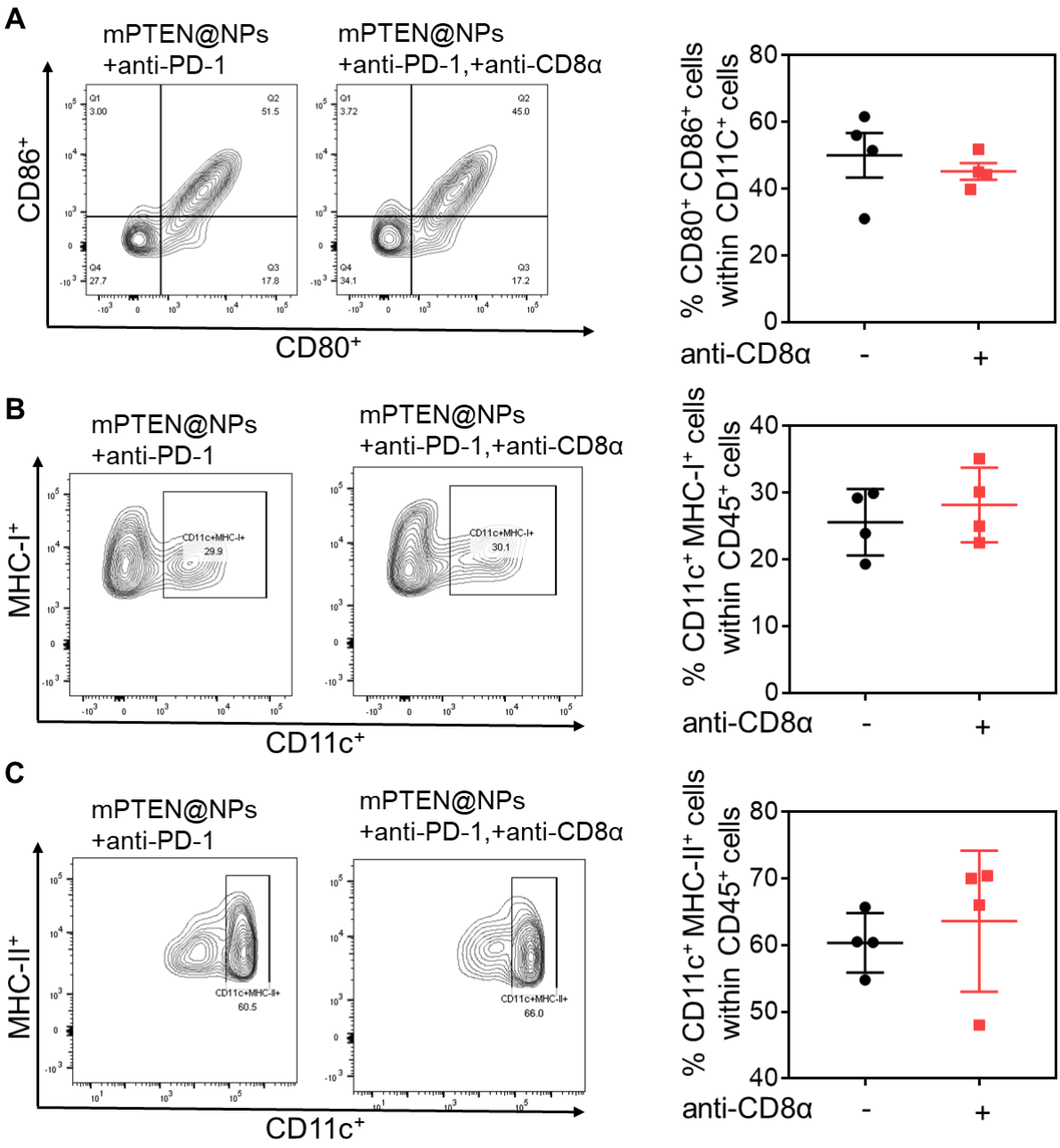

Fig. S48. Representative flow cytometric analysis and quantitation of lymph node dendritic cells after treatment of CD8$^+$ T cell-depleted, tumor-bearing mice with mPTEN@NPs. B16F10 tumor-bearing mice were euthanized and inguinal lymph node were isolated 48 hours post the third round of treatment. (**A**) Percentage of CD11c$^+$CD45$^+$ cells. (**B**) Percentage of CD80$^+$CD86$^+$ cells. (**C**) Percentage of CD11c$^+$MHC-II$^+$ cells. Data are presented as mean ± SEM (n = 4 mice per group).

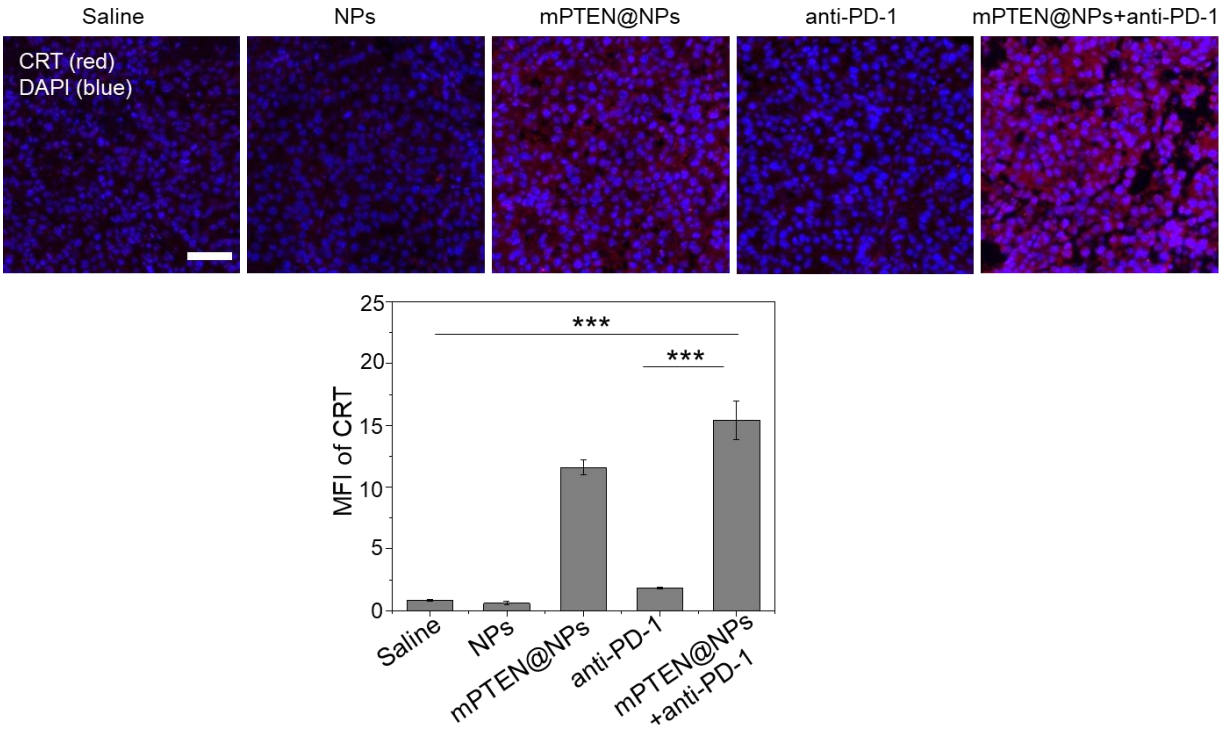

Fig. S49. Immunofluorescence staining of tumor tissues and quantitation of CRT (red) after treatment with saline (Ctrl), NPs, mPTEN@NPs, anti-PD-1, or mPTEN@NPs plus anti-PD-1. B16F10 tumor-bearing mice were euthanized and tumor tissues were isolated 48 hours post the third round of treatment. Data are presented as mean ± SD (n = 3 mice per group). Data were analyzed using a one-way ANOVA with a Tukey post-hoc test. ***P < 0.001. Scale bar, 50 μm. MFI: mean fluorescent intensity.

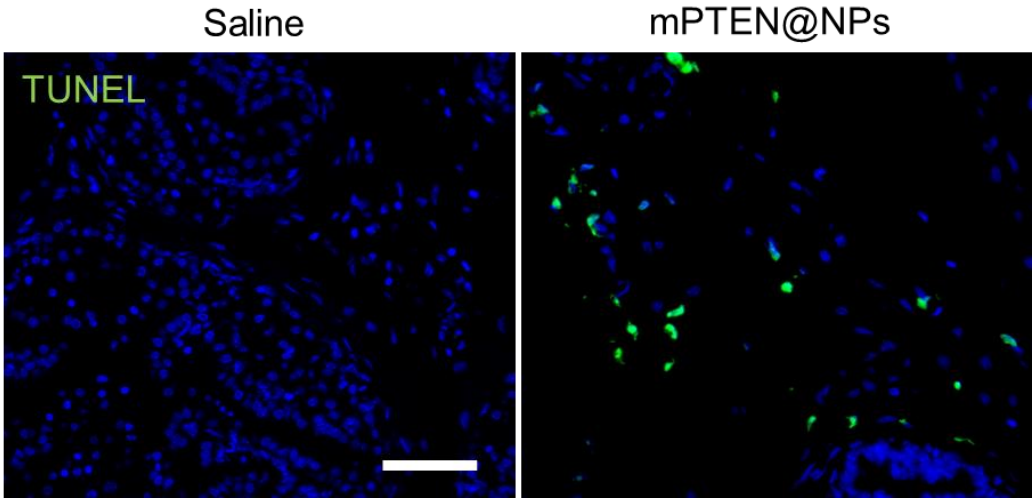

Fig. S50. TUNEL staining images of the PTEN-Cap8-bearing tumor tissues after treatment with saline (Ctrl) and mPTEN@NPs. PTEN-Cap8 tumor-bearing mice were euthanized and tumor tissues were isolated 48 hours post the third round of treatment. Scale bar, 50 μm.

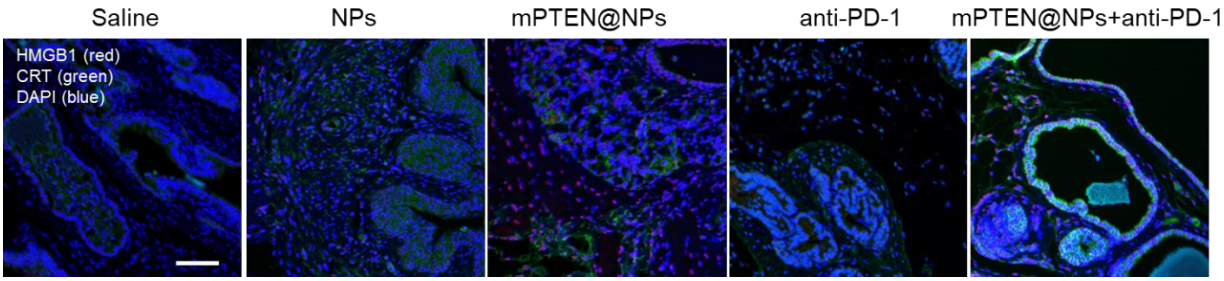

Fig. S51. Immunofluorescence staining of tumor tissues for HMGB1 and CRT expression isolated from PTEN-Cap8 tumor-bearing mice. PTEN-Cap8 tumor-bearing mice were euthanized and tumor tissues were isolated 48 hours post the third round of treatment. HMGB1 (red), CRT (green), DAPI (blue). Scale bar, 100 μm.

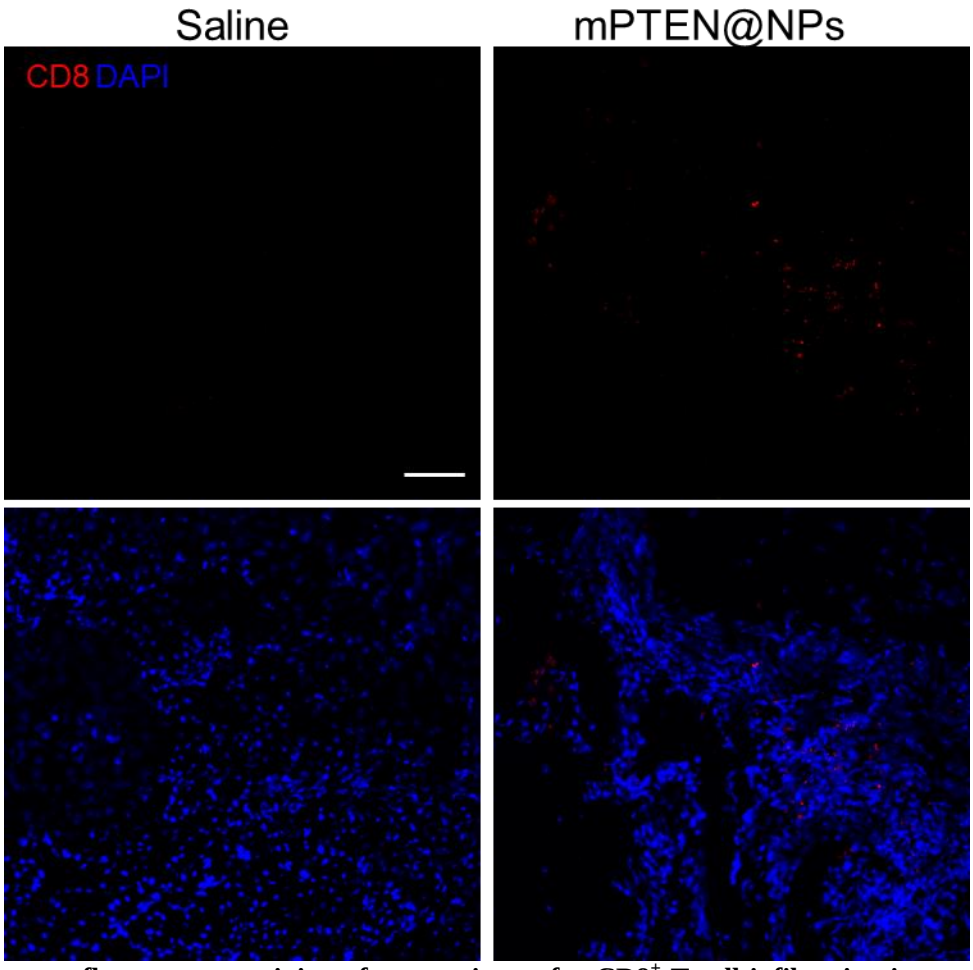

Fig. S52. Immunofluorescence staining of tumor tissues for $CD8^+$ T cell infiltration in tumors isolated from BMPC mice. BMPC were euthanized and tumor tissues were isolated 48 hours post the third round of treatment. CD8 staining are shown in red. Scale bar, 75 μm.

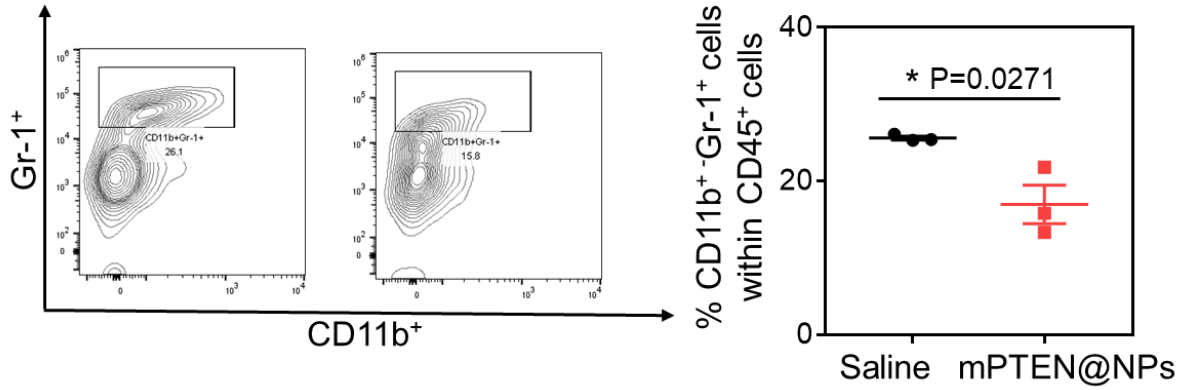

Fig. S53. Representative flow cytometric analysis and quantitation of CD11b$^+$Gr-1$^+$ myeloid-derived suppressor cells in tumors isolated from BMPC mice. BMPC were euthanized and tumor tissues were isolated 48 hours post the third round of treatment. Data are presented as mean ± SEM (n = 3 mice per group). Data were analyzed by a Student's *t*-test. *P < 0.05.

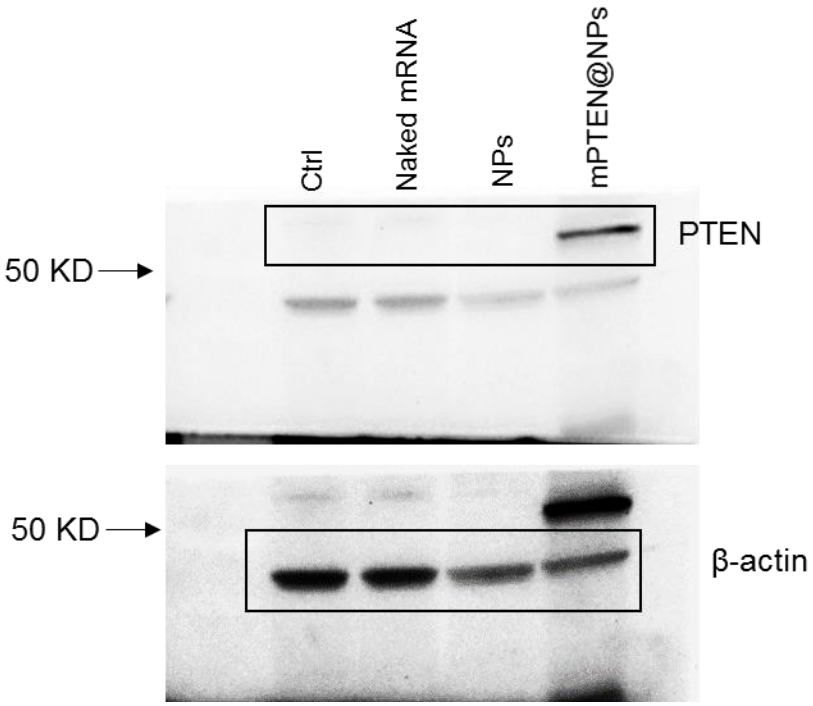

Fig. S54. Full scans of Western blots corresponding to Fig. 1G. Black lines represent the areas used in Fig. 1G.

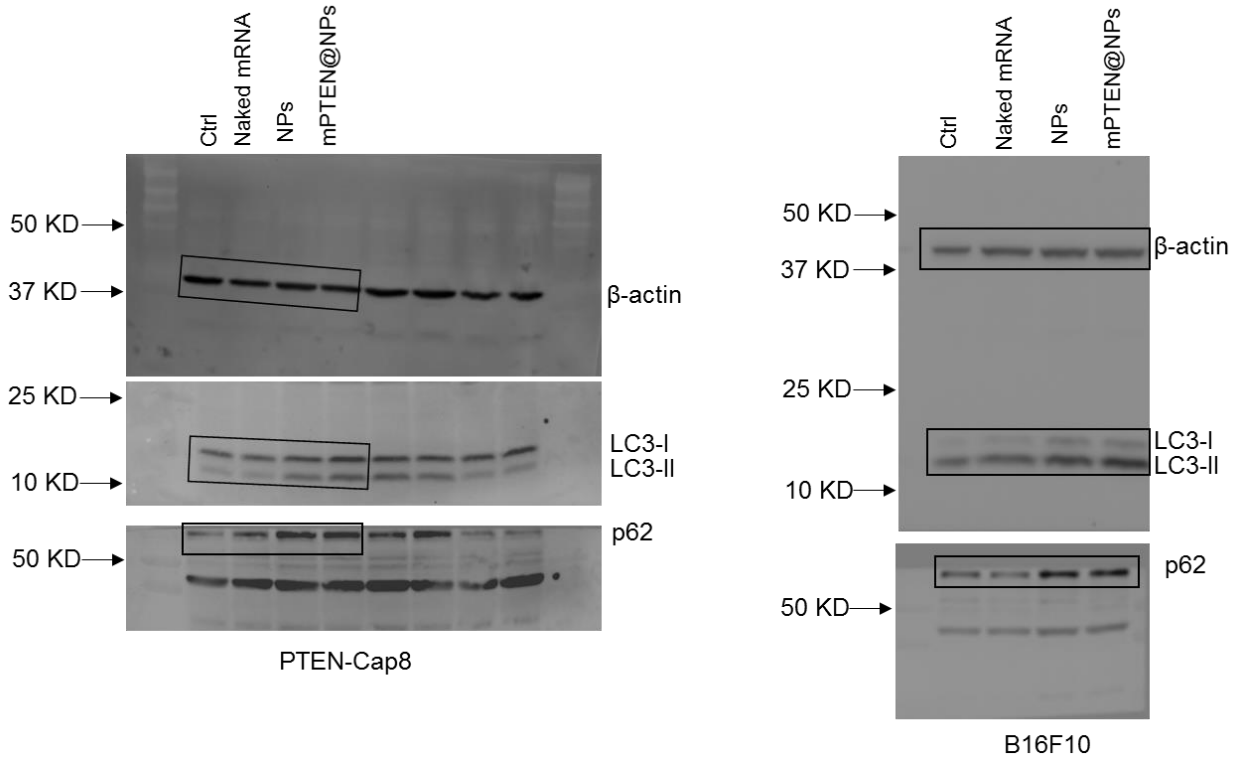

Fig. S55. Full scans of Western blots corresponding to fig. S14. Black lines represent the areas used in fig. S14.

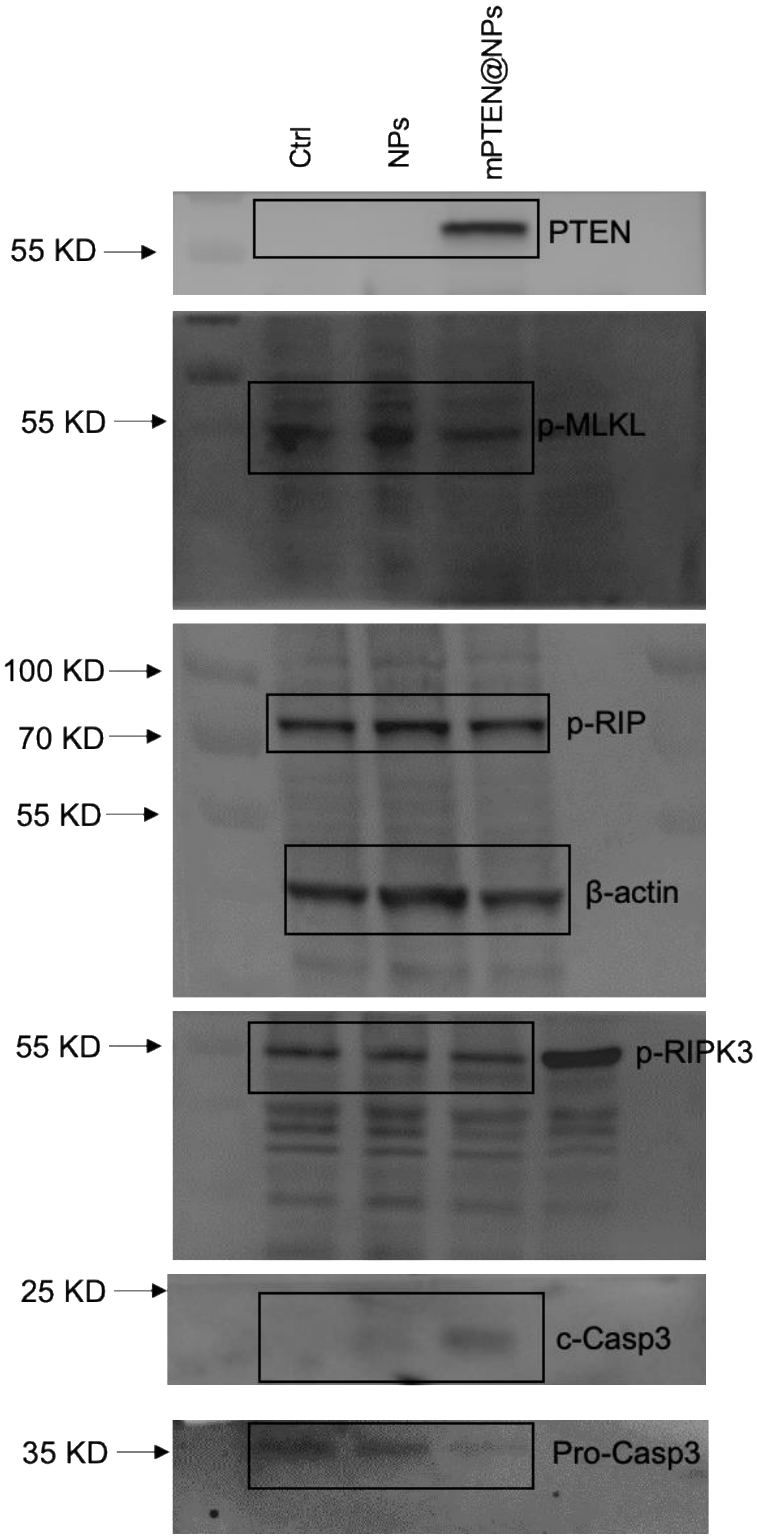

Fig. S56. Full scans of Western blots corresponding to fig. S12. Black lines represent the areas used in fig. S12.

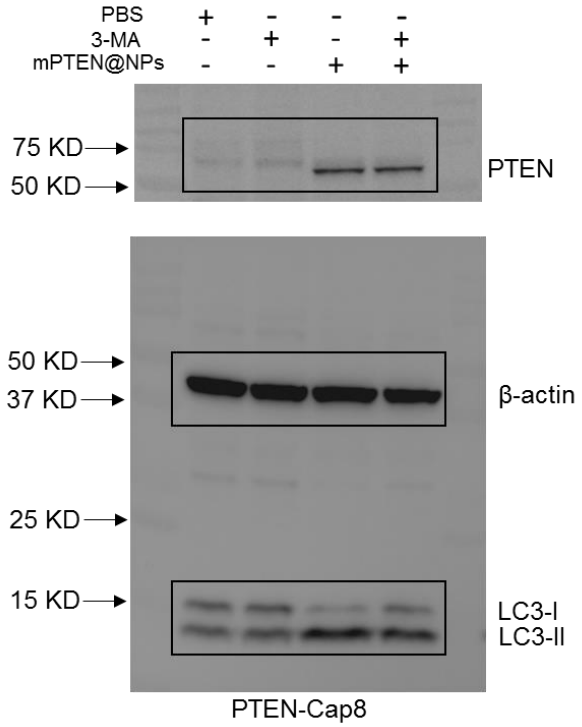

Fig. S57. Full scans of Western blots corresponding to Fig. 2G. Black lines represent the areas used in Fig. 2G.

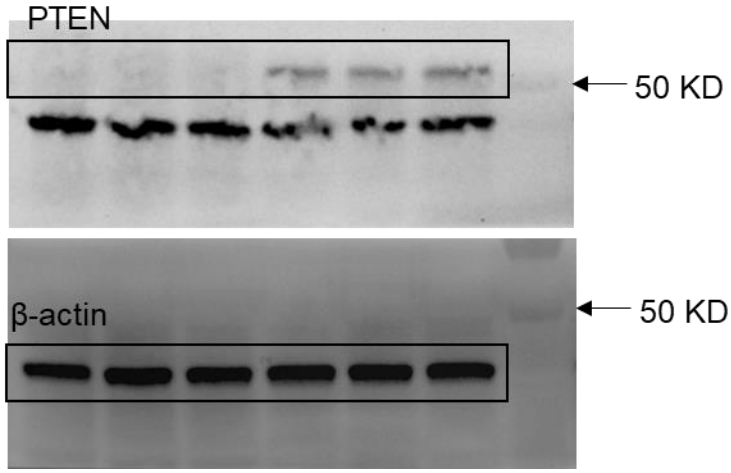

Fig. S58. Full scans of Western blots corresponding to fig. S25. Black lines represent the areas used in fig. S25.

Table S1. Biochemical analysis of mouse blood after 3 rounds of treatment.

	ALT (U/L)	AST (U/L)	BUN (mg/dL)	RBC (10^{12}/L)	WBC (10^9/L)
Reference	28-129	46-392	7-28	6.36-9.42	0.8-6.8
Saline	78.65±10.76	102.91±19.01	22.08±2.68	8.51±0.49	4.13±0.91
Control NPs	61.76±1.46	77.84±7.63	17.76±1.49	8.28±1.30	4.5±0.87
mPTEN@NPs	88.22±19.40	111.66±30.96	19.17±1.0	8.46±0.49	3.3±0.85

ALT, Alanine aminotransferase; AST, Aspartate aminotransferase; BUN, Urea nitrogen; RBC, Red blood cell; WBC, White blood cell. Data represent the mean ± SD (n = 3 mice per group).

Table S2. Antibodies for flow cytometry.

Product	Cat#	Concentration for use
PerCP/Cyanine5.5 anti-mouse CD45.2	109828	2.5 μg/mL
APC anti-mouse CD3	100236	5 μg/mL
FITC anti-mouse CD4	100405	2.5 μg/mL
PE anti-mouse CD8a	100708	2.5 μg/mL
PE anti-mouse CD25	101903	1 μg/mL
APC anti-mouse Ly-6C	128015	2.5 μg/mL
PE/Cyanine7 anti-mouse Ly-6G	127617	2.5 μg/mL
Alexa Fluor® 647 anti-mouse FOXP3	126407	1 μg/mL
APC/Cyanine7 anti-mouse H-2Kd	116629	2.5 μg/mL
PE/Cyanine7 anti-mouse I-Ab	116419	2.5 μg/mL
FITC anti-mouse/human CD11b	101206	2.5 μg/mL
APC anti-mouse CD11c	117310	2.5 μg/mL
FITC anti-mouse CD86	105005	1 μg/mL
PE anti-mouse CD80	104707	5 μg/mL
PE anti-mouse Ly-6G/Ly-6C (Gr-1)	108407	2.5 μg/mL
PE/Cyanine7 anti-mouse T-bet	644824	2.5 μg/mL
APC/Cyanine7 anti-mouse IFN-γ	505850	1.25 μg/mL